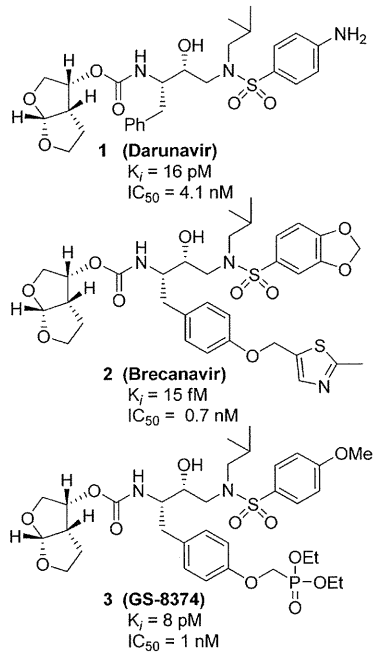

Figure 1. Structures of protease inhibitors **1**−**3**.

Scheme 1. Synthesis of Bis-THF Ligand 11

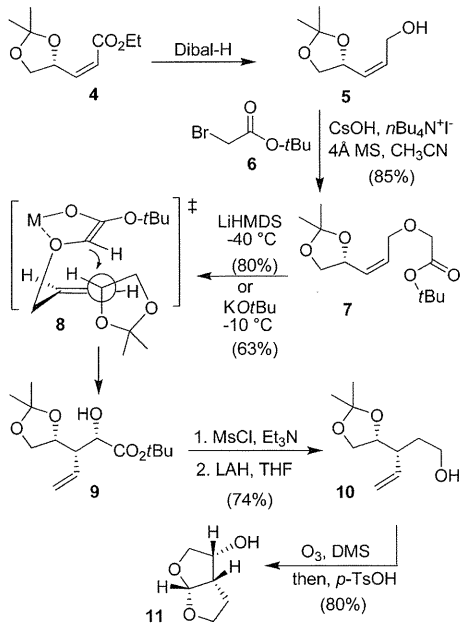

acid,[15,16] L-arabinose,[17] L-serine,[18] and L-tartaric acid,[19] as reported. We used the L-tartaric acid-derived procedure for our synthesis. Dibal-H reduction of **4** resulted in alcohol **5** (Scheme 1).[20,21]

We investigated the *O*-alkylation of **5** using *tert*-butyl bromoacetate **6** under a variety of conditions. The use of KO*t*Bu in THF at 23 °C for 2 h resulted in a single product, **7** in 56% yield. *O*-alkylation, using Cs_2CO_3 in DMF also proceeded with a moderate yield (59%). However, the use of CsOH−H_2O and activated molecular sieves, in the presence of tetrabutylammonium iodide in acetonitrile, provided the best results.[22] These conditions afforded the desired *O*-alkylated product **7** in 85% yield. Only a small amount of the transesterification product (<5%) and a small amount (<5%) of starting material were recovered in this reaction.

We then investigated a [2,3]-sigmatropic rearrangement of **7** under a variety of conditions. Reaction of **7** with KO*t*Bu at 23 °C proceeded smoothly but provided **9** a 4:1 diastereoselective ratio at the C2-chiral center. Lowering the temperature to −10 °C resulted in a marked increase in selectivity (17:1) with a moderate yield (63%). It should be noted that the C2-chiral center would be eliminated en route to the bis-THF ligand; however, stereoselectivity is important for the synthesis of C4-derivatives. Reactions with LiHMDS in THF at −20 °C provided **9** in 55% yield and 6:1 diastereoselectivity. However, the same reaction at −40 °C to −30 °C for 1 h provided the best yield. Diastereomer **9** was obtained as a single product in 80% yield. The stereochemical outcome of the [2,3]-sigmatropic rearrangement can be rationalized by the proposed transition-state model **8**, in which the allylic C−O bond is orthogonal to the plane of the allylic C=C and is antiperiplanar with respect to the approaching carbanion, as described by Bruckner and co-workers.[23] For the synthesis of the bis-THF ligand, alcohol **9** was converted to the corresponding mesylate. LAH reduction of the mesylate provided alcohol **10** in 74% yield, over 2 steps. Oxidative cleavage of the terminal alkene followed by acid-catalyzed cyclization, in the presence of a catalytic amount of *p*-TsOH in $CHCl_3$ at reflux, afforded the bis-THF alcohol **11** in 80% yield.

Scheme 2. Syntheses of Substituted Bis-THF Ligands

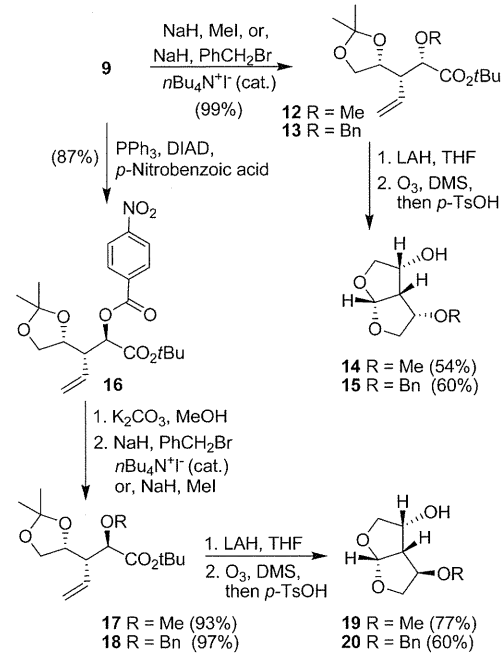

As shown in Scheme 2, rearrangement product **9** was utilized for the synthesis of C4-substituted bis-THF ligands. Alcohol **9** can be conveniently functionalized into derivatives which can further interact with the HIV-1 protease backbone atoms. Thus, protection of the free hydroxyl group provided methyl and benzyl ethers **12** and **13**, respectively. LAH reduction, followed by ozonolysis, and acid-catalyzed cyclization resulted in compounds **14** and **15**, respectively. Inversion of the C2-hydroxyl group of **9** using Mitsunobu's protocol[24] gave **16** in 87% yield.

dx.doi.org/10.1021/ml100289m |*ACS Med. Chem. Lett.* 2011, 2, 298–302

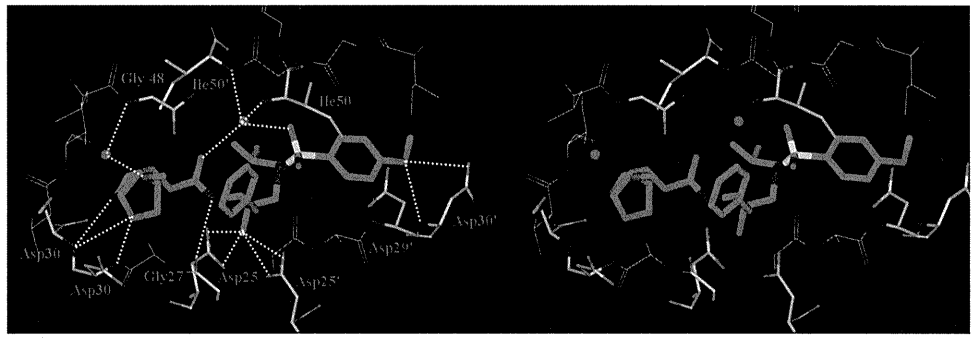

Figure 2. Stereoview of the X-ray structure of inhibitor **23c** (green)-bound HIV-1 protease (pdb code: 3QAA). All strong hydrogen bonding interactions are shown as dotted lines.

Scheme 3. Syntheses of Protease Inhibitors

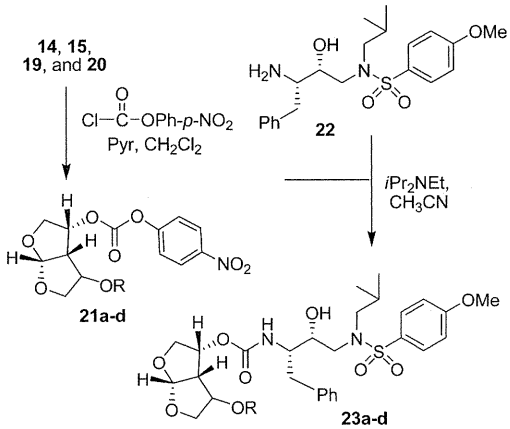

Selective deprotection of the nitro benzoate with potassium carbonate in methanol at 0 °C, and subsequent protection with methyl iodide or benzyl bromide provided methyl and benzyl ethers **17** and **18**, respectively. LAH reduction, ozonolysis, and cyclization resulted in the desired substituted bis-THF ligands **19** and **20**.

As shown in Scheme 3, alcohols **14**, **15**, **19**, and **20** were activated with *p*-nitrophenyl chloroformate to provide mixed activated carbonates **21a**–**d**. These carbonates were reacted with amine **22** to afford HIV-1 protease inhibitors **23a**–**d**.[8] These inhibitors were all evaluated for their activity in both enzyme inhibitory and antiviral assays. The results are shown in Table 1. The enzyme inhibitory activity (K_i) was determined according to an assay protocol reported by Toth and Marshall.[25] The inhibitors displayed extremely potent enzyme inhibitory activity. Compound **23c** (K_i = 0.0029 nM) is the most potent compound in this series. Its diastereomer **23a** (K_i = 0.035 nM) displayed a loss in enzyme inhibitory activity. The benzyl derivatives **23b** and **23d** have also shown reduced enzyme activity. Antiviral IC_{50} values were determined using the MTT assay.[26,27] Consistent with its enzyme inhibitory potency, inhibitor **23c** exhibited an impressive antiviral activity (IC_{50} = 2.4 nM).

To gain molecular insights into ligand-binding site interactions responsible for the potent antiviral activity of inhibitor **23c**, we have determined an X-ray crystal structure of GRL-04410 (**23c**) complexed with the wild-type protease. The structure was refined to an *R*-factor of 0.175 at a high resolution of 1.40 Å. The structure comprises the protease dimer and inhibitor in two orientations related by a 180° rotation, with 55/45 relative

Table 1. Structure and Activity of Inhibitors

Entry	Inhibitor	K_i (nM)	IC_{50}(nM)[a,b]
1.	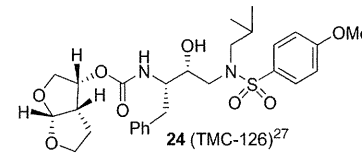 **24** (TMC-126)[27]	0.014	1.4
2.	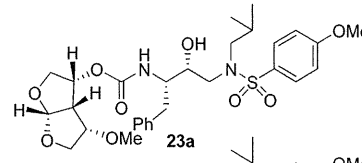 **23a**	0.035	55
3.	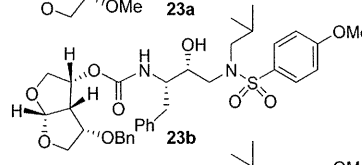 **23b**	0.073	335
4.	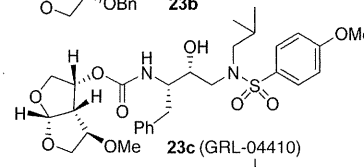 **23c** (GRL-04410)	0.0029	2.4
5.	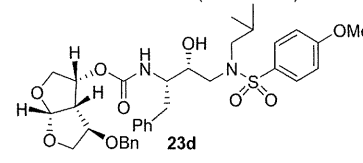 **23d**	0.3	---

[a] Values are means of at least three experiments. [b] Human T-lymphoid (MT-2) cells were exposed to 100 $TCID_{50}$ values of HIV-1_{LAI} and cultured in the presence of each PI, and IC_{50} values were determined using the MTT assay.

occupancies (pdb code: 3QAA). The protease dimer structure is essentially identical to that in the protease–darunavir complex with a rmsd of 0.14 Å on the Cα atoms.[28] The inhibitor interactions in the active site cavity consist of a series of hydrogen bonds and weaker CH···O interactions, as described previously for darunavir and GRL-09865.[28,29] The critical differences are provided by the methoxy group on the bis-THF ligand in **23c**. As shown in Figure 2, the methoxy oxygen forms a water-mediated hydrogen bond with the amide NH of Gly-48. Furthermore, the methyl group forms a CH···O interaction with the carbonyl oxygen of Gly-48 that could stabilize the conformation of the flexible flaps. The flexibility of the flaps is important for the binding of substrates or inhibitors and for the catalytic activity of HIV protease. The flap conformation and flexibility

can be altered by sequence polymorphisms and drug resistant mutations.[30−32] Consequently, inhibitors such as **23c** with strong flap interactions are expected to retain high affinity for drug resistant variants of the protease.

In conclusion, we investigated C4-alkoxy substituted bis-THF-derived HIV-1 protease inhibitors in order to enhance ligand-binding site interactions in the HIV-1 protease active site. In this context, we have developed an optically active synthesis of the bis-THF and C4-substituted bis-THF ligands using a [2,3]-sigmatropic rearrangement as the key step. Incorporation of C4-substituted bis-THF ligands resulted in a series of highly potent HIV protease inhibitors. Compound **23c** is remarkably potent (K_i = 2.9 pM; IC_{50} = 2.4 nM). The stereochemical importance of the methoxy substituent is evident, as the corresponding epimer is significantly less potent. A protein−ligand X-ray structure of **23c**-bound HIV-1 protease revealed extensive interactions of the inhibitor in the active site of HIV-1 protease. It maintained all key backbone hydrogen bonding interactions similar to those of darunavir. Of particular importance, the methoxy oxygen on the bis-THF ligand is involved in a unique water-mediated hydrogen bond to the Gly-48 amide NH. Further design and ligand optimization involving this interaction is in progress.

■ ASSOCIATED CONTENT

Supporting Information. Experimental procedures and ^{1}H- and ^{13}C-NMR spectral data for all new compounds. This material is available free of charge via the Internet at http://pubs.acs.org.

■ AUTHOR INFORMATION

Corresponding Author

*E-mail: akghosh@purdue.edu (A.K.G.).

Funding Sources

Financial support by the National Institutes of Health (GM 53386, A.K.G.; GM 062920, I.T.W.) is gratefully acknowledged. This work was also supported in part by the Intramural Research Program of the Center for Cancer Research, National Cancer Institute, National Institutes of Health, and in part by a Grant-in-aid for Scientific Research (Priority Areas) from the Ministry of Education, Culture, Sports, Science, and Technology of Japan (Monbu Kagakusho) and a Grant for Promotion of AIDS Research from the Ministry of Health, Welfare, and Labor of Japan.

■ ACKNOWLEDGMENT

We thank the staff at the Southeast Regional-Collaborative Access Team (SER-CAT) at the Advanced Photon Source, Argonne National Laboratory, for assistance during X-ray data collection. Use of the Advanced Photon Source was supported by the U.S. Department of Energy, Office of Science, Office of Basic Energy Sciences, under Contract No. W-31-109-Eng-38. We thank Drs. K. V. Rao and Bruno Chapsal (Purdue University) for helpful discussions.

■ REFERENCES

(1) Ghosh, A. K. Harnessing Nature's Insight: Design of Aspartyl Protease Inhibitors from Treatment of Drug-Resistant HIV to Alzheimer's Disease. *J. Med. Chem.* **2009**, *52*, 2163–2176.

(2) FDA approves Darunavir on June 23, 2006: FDA approved a new HIV treatment for patients who do not respond to existing drugs. Please see http://www.fda.gov/bbs/topics/NEWS/2006/NEW01395.html.

(3) On October 21, 2008, FDA granted traditional approval to Prezista (darunavir), coadministered with ritonavir and with other antiretroviral agents, for the treatment of HIV-1 infection in treatment-experienced adult patients. In addition, a new dosing regimen for treatment-naïve adult patients was approved.

(4) Ghosh, A. K.; Sridhar, P. R.; Kumaragurubaran, N.; Koh, Y.; Weber, I. T.; Mitsuya, H. A Privileged Ligand for Darunavir and a New Generation of HIV-Protease Inhibitors That Combat Drug-Resistance. *ChemMedChem* **2006**, *1*, 939–950.

(5) Ghosh, A. K.; Chapsal, B. D.; Weber, I. T.; Mitsuya, H. Design of HIV Protease Inhibitors Targeting Protein Backbone: An Effective Strategy for Combating Drug Resistance. *Acc. Chem. Res.* **2008**, *41*, 78–86.

(6) Miller, J. F.; Andrews, C. W.; Brieger, M.; Furfine, E. S.; Hale, M. R.; Hanlon, M. H.; Hazen, R. J.; Kaldor, I.; McLean, E. W.; Reynolds, D.; Sammond, D. M.; Spaltenstein, A.; Tung, R.; Turner, E. M.; Xu, R. X.; Sherrill, R. G. Ultra-potent P1 modified arylsulfonamide HIV protease inhibitors: The discovery of GW0385. *Bioorg. Med. Chem. Lett.* **2006**, *16*, 1788–1794.

(7) Chilar, T.; He, G.-X.; Kiu, X.; Chen, J.; Hatada, M.; Swaminathan, S.; McDermott, M. J.; Yang, Z.-Y.; Mulato, A. S.; Chen, X.; Leavitt, S. A.; Stray, K. M.; Lee, W. A. Suppression of HIV-1 Protease Inhibitor Resistance by Phosphonate-mediated Solvent Anchoring. *J. Mol. Biol.* **2006**, *363*, 635–647.

(8) Ghosh, A. K.; Martyr, C. D. Darunavir (Prezista): A HIV-1 Protease Inhibitor for Treatment of Multidrug-Resistant HIV; Li, J. J., Johnson, D. S., Eds.; In *Modern Drug Synthesis*; Wiley: Hoboken, New Jersey, 2010; pp 29−44.

(9) Ghosh, A. K.; Chen, Y. Synthesis and Optical Resolution of High Affinity P2-Ligands for HIV-1 Protease Inhibitors. *Tetrahedron Lett.* **1995**, *36*, 505–508.

(10) Ghosh, A. K.; Kincaid, J. F.; Walters, D. E.; Chen, Y.; Chaudhuri, N. C.; Thompson, W. J.; Culberson, C.; Fitzgerald, P. M. D.; Lee, H. Y.; McKee, S. P.; Munson, P. M.; Duong, T. T.; Darke, P. L.; Zugay, J. A.; Schleif, W. A.; Axel, M. G.; Lin, J.; Huff, J. R. Nonpeptidal P2-Ligands for HIV Protease Inhibitors: Structure-Based Design, Synthesis and Biological Evaluations. *J. Med. Chem.* **1996**, *39*, 3278–3290.

(11) Ghosh, A. K.; Leshchenko, S.; Noetzel, M. Stereoselective Photochemical 1,3-Dioxolane Addition to α,β Unsaturated-γ-lactone: Synthesis of Bis-tetrahydrofuranyl Ligand for HIV Protease Inhibitor UIC-94-017 (TMC-114). *J. Org. Chem.* **2004**, *69*, 7822–7829.

(12) Ghosh, A. K.; Li, J.; Perali, R. S. A Stereoselective Anti-aldol Route to (3*R*,3a*S*,6a*R*)-Tetrahydro-2*H*-furo[2,3-*b*]furan-3-ol: A Key Ligand for a New Generation of HIV Protease Inhibitors. *Synthesis* **2006**, 3015–3018.

(13) Quaedflieg, P. J. L. M.; Kesteleyn, B. R. R.; Wigerinck, P. B. T. P.; Goyvaerts, N. M. F.; Jan Vijn, R.; Liebregts, C. S. M.; Kooistra, J. H. M. H.; Cusan, C. Stereoselective and Efficient Synthesis of (3*R*,3a*S*,6a*R*)-Hexahydrofuro[2,3-*b*]furan-3-ol. *Org. Lett.* **2005**, *7*, 5917–5920.

(14) Black, D. M.; Davis, R.; Doan, B. D.; Lovelace, T. C.; Millar, A.; Toczko, J. F.; Xie, S. Highly diastereo- and enantioselective catalytic synthesis of the bis-tetrahydrofuran alcohol of Brecanavir and Darunavir. *Tetrahedron: Asymmetry* **2008**, *19*, 2015–2019.

(15) Andrews, G. C.; Crawford, T. C.; Bacon, B. E. Stereoselective, catalytic reduction of L-ascorbic acid: a convenient synthesis of L-gulono-1,4-lactone. *J. Org. Chem.* **1981**, *46*, 2977–2979.

(16) Hubschwerlen, C.; Specklin, J.-L.; Higelin, J. L-(*S*)-Glyceraldehyde Acetonide. *Organic Syntheses*; Wiley & Sons: New York, 1998; Coll Vol. No. IX, p 454.

(17) Maloneyhuss, K. E. A Useful Preparation of L-(*S*)-Glyceraldehyde Acetonide. *Synth. Commun.* **1985**, *15*, 273–277.

(18) Hirth, G.; Walther, W. Synthesis of the (*R*)- and (*S*)-Glycerol Acetonides. Determination of the Optical Purity. *Helv. Chim. Acta* **1985**, *68*, 1863–1871.

(19) Al-Hakim, A. H.; Haines, A. H.; Morley, C. Synthesis of 1,2-*O*-Isopropylidene-L-threitol and its Conversion to (*R*)-1,2-*O*-Isopropylideneglycerol. *Synthesis* **1985**, *2*, 207–208.

(20) Mann, J.; Weymouth-Wilson, A. C. Photoinduced-Addition of Methanol to (5*S*)-(5-*O*-tert-Butyldimethylsiloxymethyl)Furan-2(5*H*)-one: (4*R*,5*S*)-4-Hydroxymethyl-(5-*O*-*tert*-Butyldimethyl siloxymethyl) Furan-2(5*H*)-one. *Organic Syntheses*; Wiley & Sons: New York, 2004; Collect. Vol. No. X, p 152; 1998.

(21) Borcherding, D. R.; et al. Potential inhibitors of *S*-adenosylmethionine-dependent methyltransferases. Molecular dissections of neplanocin A as potential inhibitors of *S*-adenosylhomocysteine hydrolase. *J. Med. Chem.* **1988**, *31*, 1729–1738.

(22) Dueno, E. E.; Chu, F.; Kim, S.-I.; Jung, K. W. Cesium promoted *O*-alkylation of alcohols for the efficient ether synthesis. *Tetrahedron Lett.* **1999**, *40*, 1843–1846.

(23) Brückner, R.; Priepke, H. Asymmetric Induction in the [2,3]-Wittig Rearrangement by Chiral Substituents in the Allyl Moiety. *Angew. Chem., Int. Ed. Engl.* **1988**, *27*, 278–280.

(24) Dodge, J. A.; Nissen, J. S.; Presnell, M. A General Procedure for Mitsunobu Inversion of Sterically Hindered Alcohols: Inversion of Menthol. (1*S*,2*S*,5*R*)-5-Methyl-2-(1-Methylethyl)Cyclohexyl 4-Nitrobenzoate. *Organic Syntheses*; Wiley & Sons: New York, 1998; Collect. Vol. No. IX, pp 607−611.

(25) Toth, M. V.; Marshall, G. R. A simple, continuous fluorometric assay for HIV protease. *Int. J. Pept. Protein Res.* **1990**, *36*, 544–550.

(26) Koh, Y.; Nakata, H.; Maeda, K.; Ogata, H.; Bilcer, G.; Devasamudram, T.; Kincaid, J. F.; Boross, P.; Wang, Y.-F.; Tie, Y.; Volarath, P.; Gaddis, L.; Harrison, R. W.; Weber, I. T.; Ghosh, A. K.; Mitsuya, H. A Novel bis-Tetrahydrofuranylurethane-containing Nonpeptide Protease Inhibitor (PI) UIC-94017 (TMC114) Potent Against Multi-PI-Resistant HIV In Vitro. *Antimicrob. Agents Chemother.* **2003**, *47*, 3123–3129.

(27) Yoshimura, K.; Kato, R.; Kavlick, M. F.; Nguyen, A.; Maroun, V.; Maeda, K.; Hussain, K. A.; Ghosh, A. K.; Gulnik, S. V.; Erickson, J. W.; Mitsuya, H. UIC-94003: A Potent Protease Inhibitor (PI) That Inhibits Multi-PI-Resistant HIV-1 Replication in vitro. *J. Virol.* **2002**, *76*, 1349–1358.

(28) Tie, Y.; Boross, P. I.; Wang, Y. F.; Gaddis, L.; Hussain, A. K.; Leshchenko, S.; Ghosh, A. K.; Louis, J. M.; Harrison, R. W.; Weber, I. T. High Resolution Crystal Structures of HIV-1 Protease with a Potent Non-Peptide Inhibitor (UIC-94017) Active Against Multi-Drug-Resistant Clinical Strains. *J. Mol. Biol.* **2004**, *338*, 341–352.

(29) Wang, Y. F.; Tie, Y.; Boross, P. I.; Tozser, J.; Ghosh, A. K.; Harrison, R. W.; Weber, I. T. Potent new antiviral compound shows similar inhibition and structural interactions with drug resistant mutants and wild type HIV-1 protease. *J. Med. Chem.* **2007**, *50*, 4509–4515.

(30) Kear, J. L.; Blackburn, M. E.; Veloro, A. M.; Dunn, B. M.; Fanucci, G. E. Subtype polymorphisms among HIV-1 protease variants confer altered flap conformations and flexibility. *J. Am. Chem. Soc.* **2009**, *131*, 14650–14651.

(31) Coman, R. M.; Robbins, A. H.; Goodenow, M. M.; Dunn, B. M.; McKenna, R. High-resolution structure of unbound human immunodeficiency virus 1 subtype C protease: implications of flap dynamics and drug resistance. *Acta Crystallogr., D: Biol. Crystallogr.* **2008**, *D64*, 754–763.

(32) Liu, F.; Kovalevsky, A. Y.; Louis, J. M.; Boross, P. I.; Wang, Y. F.; Harrison, R. W.; Weber, I. T. Mechanism of drug resistance revealed by the crystal structure of the unliganded HIV-1 protease with F53L mutation. *J. Mol. Biol.* **2006**, *358*, 1191–1199.

ANTIMICROBIAL AGENTS AND CHEMOTHERAPY, Apr. 2011, p. 1717–1727 Vol. 55, No. 4
0066-4804/11/$12.00 doi:10.1128/AAC.01540-10

Novel HIV-1 Protease Inhibitors (PIs) Containing a Bicyclic P2 Functional Moiety, Tetrahydropyrano-Tetrahydrofuran, That Are Potent against Multi-PI-Resistant HIV-1 Variants[▽]†

Kazuhiko Ide,[1] Manabu Aoki,[1,2] Masayuki Amano,[1] Yasuhiro Koh,[1] Ravikiran S. Yedidi,[3] Debananda Das,[3] Sofiya Leschenko,[4] Bruno Chapsal,[4] Arun K. Ghosh,[4] and Hiroaki Mitsuya[1,3]*

Departments of Hematology, Rheumatology, and Infectious Diseases, Kumamoto University Graduate School of Medicine, Kumamoto 860-8556, Japan[1]; Department of Medical Technology, Kumamoto Health Science University, Kumamoto 861-5598, Japan[2]; Experimental Retrovirology Section, HIV and AIDS Malignancy Branch, National Cancer Institute, National Institutes of Health, Bethesda, Maryland 20892[3]; and Departments of Chemistry and Medicinal Chemistry, Purdue University, West Lafayette, Indiana 47907[4]

Received 8 November 2010/Returned for modification 13 December 2010/Accepted 19 January 2011

We identified GRL-1388 and -1398, potent nonpeptidic human immunodeficiency virus type 1 (HIV-1) protease inhibitors (PIs) containing a bicyclic P2 functional moiety, tetrahydropyrano-tetrahydrofuran (Tp-THF). GRL-1388 was as potent as darunavir (DRV) against various drug-resistant HIV-1 laboratory strains with 50% effective concentration (EC_{50}s) of 2.6 to 32.6 nM. GRL-1398 was significantly more potent against such variants than DRV with EC_{50}s of 0.1 to 5.7 nM. GRL-1388 and -1398 were also potent against multiple-PI-resistant clinical HIV-1 variants ($_{CL}$HIV-1_{MDR}) with EC_{50}s ranging from 2.7 to 21.3 nM and from 0.3 to 4.8 nM, respectively. A highly DRV-resistant HIV-1 variant selected *in vitro* remained susceptible to GRL-1398 with the EC_{50} of 21.9 nM, while the EC_{50} of DRV was 214.1 nM. When HIV-1_{NL4-3} was selected with GRL-1398, four amino acid substitutions—leucine to phenylalanine at a position 10 (L10F), A28S, L33F, and M46I—emerged, ultimately enabling the virus to replicate in the presence of >1.0 μM the compound beyond 57 weeks of selection. When a mixture of 10 different $_{CL}$HIV-1_{MDR} strains was selected, the emergence of resistant variants was more substantially delayed with GRL-1398 than with GRL-1388 and DRV. Modeling analyses revealed that GRL-1398 had greater overall hydrogen bonding and hydrophobic interactions than GRL-1388 and DRV and that GRL-1388 and -1398 had hydrogen bonding interactions with the main chain of the active-site amino acids (Asp29 and Asp30) of protease. The present findings warrant that GRL-1398 be further developed as a potential drug for treating individuals with HIV-1 infection.

Currently available combination therapy or highly active antiretroviral therapy (HAART) has been shown to suppress the replication of human immunodeficiency virus type 1 (HIV-1) and significantly extend the life expectancy of HIV-1-infected individuals (20, 33). However, the ability to provide effective long-term antiretroviral therapy for HIV-1 infection remains a complex issue since the reverse transcriptase of HIV-1 is error-prone, and the replication rate of the virus is enormously rapid, thus enabling HIV-1 to eventually develop resistance to virtually any existing antiretroviral agents. Therefore, continuous efforts are required to develop more potent and safer therapeutics of a different structure(s), mechanism(s), and/or class(es) with a high genetic barrier against HIV-1's acquisition of drug resistance.

HIV-1 protease inhibitors (PIs) are one of the most often used classes of antiretroviral drugs in HAART. Darunavir (DRV), the latest addition among currently available PIs, contains a unique nonpeptidic P2 functional group, *bis*-tetrahydrofuranylurethane (*bis*-THF), exerts greatly potent activity against a wide spectrum of laboratory and clinical multidrug-resistant HIV-1 variants (HIV-1_{MDR}). We have previously reported that the high efficacy and genetic barrier of DRV should be associated with its dual antiviral activity: (i) protease enzymatic inhibition and (ii) protease dimerization inhibition (18, 19).

In the present work, we designed, synthesized, and evaluated nonpeptidic HIV-1 protease inhibitors, GRL-1388 and -1398, which contain a novel bicyclic P2 functional group, tetrahydropyrano-tetrahydrofuran (Tp-THF), instead of the *bis*-THF moiety of DRV, and show highly potent antiretroviral activity against not only wild-type HIV-1 but also a variety of multi-PI-resistant laboratory HIV-1 strains, including a highly DRV-resistant HIV-1 variant, selected against DRV *in vitro* as recently described (17), and various multidrug-resistant clinical isolates. Structural modeling analyses revealed that the Tp-THF moiety of GRL-1388 and -1398 forms effective and strong hydrogen bond interactions with the main chain atoms of the protease active site amino acids, as does the *bis*-THF moiety of DRV. In particular, the additional polar and hydrophobic interactions between GRL-1398 and HIV-1 protease should be an explanation of its greater potency compared to that of GRL-1388.

MATERIALS AND METHODS

Cells and viruses. $CD4^+$ MT-2 and MT-4 cell lines were grown in RPMI 1640-based culture medium supplemented with 10% fetal calf serum (PAA

* Corresponding author. Mailing address: Department of Infectious Diseases and Department of Hematology, Kumamoto University School of Medicine, 1-1-1 Honjo, Kumamoto 860-8556, Japan. Phone: (81) 96-373-5156. Fax: (81) 96-363-5265. E-mail: hmitsuya@helix.nih.gov.

† Supplemental material for this article may be found at http://aac.asm.org/.

▽ Published ahead of print on 31 January 2011.

Laboratories GmbH, Linz, Austria) plus 50 U of penicillin and 100 μg of kanamycin per ml. The following HIV-1 strains were used for the drug susceptibility assay: HIV-1_{LAI}, HIV-1_{NL4-3}, a clinical HIV-1 strain isolated from a treatment-naive AIDS patient (HIV-$1_{ERS104pre}$) (28), and six HIV-1 clinical isolates that were originally isolated from patients with AIDS, who had received long-term antiretroviral therapy using 9 to 11 anti-HIV-1 drugs (without DRV) over 32 to 83 months and were genotypically and phenotypically characterized as clinical multiple-PI-resistant HIV-1 variants ($_{CL}$HIV-1_{MDR}) (36, 37). Ten such $_{CL}$HIV-1_{MDR} strains were used as follows: $_{CL}$HIV-$1_{MDR/A}$, $_{CL}$HIV-$1_{MDR/B}$, $_{CL}$HIV-$1_{MDR/C}$, $_{CL}$HIV-$1_{MDR/EV}$, $_{CL}$HIV-$1_{MDR/G}$, $_{CL}$HIV-$1_{MDR/TM}$, $_{CL}$HIV-$1_{MDR/MM}$, $_{CL}$HIV-$1_{MDR/JSL}$, $_{CL}$HIV-$1_{MDR/SS}$, and $_{CL}$HIV-$1_{MDR/13-52}$.

Antiviral agents. Nonpeptidic PIs, GRL-1388 and -1398 (Fig. 1) (molecular weights of 591.7 and 606.7, respectively), both of which contain a polycyclic ligand (Tp-THF) in place of *bis*-THF of DRV, were synthesized. The method of synthesis of GRL-1388 and -1398 will be published elsewhere by A. K. Ghosh et al. Saquinavir (SQV) and ritonavir (RTV) were kindly provided by Roche Products, Ltd. (Welwyn Garden City, United Kingdom), and Abbott Laboratories (Abbott Park, IL), respectively. Amprenavir (APV) was kindly provided by GlaxoSmithKline (Research Triangle Park, NC). Nelfinavir (NFV) and lopinavir (LPV) were kindly provided by Japan Energy, Inc., Tokyo, Japan. Atazanavir (ATV) was kindly provided by Bristol-Myers Squibb (New York, NY). Darunavir (DRV) was synthesized as previously described (16).

Drug susceptibility assay. The susceptibility of HIV-1_{LAI} to various drugs was determined as previously described (36), with minor modifications. Briefly, MT-2 cells (2×10^4/ml) were exposed to 100 50% tissue culture infective doses ($TCID_{50}$s) of HIV-1_{LAI} in the presence or absence of various concentrations of drugs in 96-well microtiter culture plates, followed by incubation at 37°C for 7 days. After 100 μl of the culture medium was removed from each well, 3-(4,5-dimetylthiazol-2-yl)-2,5-diphenyltetrazolium bromide (MTT) solution (10 μl, 7.5 mg/ml in phosphate-buffered saline) was added to each well, followed by incubation at 37°C for 3 h. After incubation to dissolve the formazan crystals, 100 μl of acidified isopropanol containing 4% (vol/vol) Triton X-100 was added to each well, and the optical density was measured by using a kinetic microplate reader (Vmax; Molecular Devices, Sunnyvale, CA). All assays were performed in duplicate or triplicate. To determine the drug sensitivity of laboratory HIV-1 strains, MT-4 cells were used as target cells. In brief, MT-4 cells (10^5/ml) were exposed to 50 $TCID_{50}$s of HIV-1_{NL4-3} and PI-resistant HIV-1 strains in the presence or absence of various concentrations of drugs, the supernatants were harvested on day 7 of culture, and the amount of p24 Gag protein were determined by using a fully automated chemiluminescent enzyme immunoassay system (Lumipulse F; Fujirebio, Inc., Tokyo, Japan) (22). To determine the susceptibility of primary HIV-1 isolates to drugs, phytohemagglutinin-activated peripheral blood mononuclear cells (PHA-PBMCs; 10^6/ml) were exposed to 50 $TCID_{50}$s of HIV-$1_{ERS104pre}$ or each $_{CL}$HIV-1_{MDR} isolate in the presence or absence of various concentrations of drugs and incubated for 7 days. Upon the conclusion of the culture, the amounts of p24 Gag protein in the supernatants were quantified. The drug concentrations that suppressed the production of p24 Gag protein by 50% (50% effective concentrations [EC_{50}s]) were determined. The p24 Gag amounts were compared to the amounts of those produced in drug-free control cell cultures. All assays were performed in duplicate or triplicate.

Generation of FRET-based HIV-1 expression system. The intermolecular fluorescence resonance energy transfer (FRET)-based HIV-1 expression assay (FRET/HIV-1 assay) using cyan and yellow fluorescent protein-tagged protease monomers (CFP and YFP, respectively) was performed as previously described (18). In brief, CFP- and YFP-tagged HIV-1 protease constructs were generated by using BD Creator DNA cloning kits (BD Biosciences, San Jose, CA). For the generation of full-length molecular infectious clones containing CFP- or YFP-tagged protease, the PCR-mediated recombination method was used (7). A linker consisting of five alanines was inserted between the protease and the fluorescent proteins. The phenylalanine-proline site that HIV-1 protease cleaves was also introduced between the fluorescent protein and reverse transcriptase sites. The DNA fragments obtained were subsequently joined by using the PCR-mediated recombination reaction performed under the standard conditions for Ex *Taq* polymerase (Takara Bio, Inc., Otsu, Japan). The amplified PCR products were cloned into the pCR-XL-TOPO vector according to the manufacturer's instructions (Gateway cloning system; Invitrogen, Carlsbad, CA). PCR products were generated with the pCR-XL-TOPO vector and used as templates, followed by digestion by both ApaI and SmaI, and the ApaI-SmaI fragment was introduced into pHIV-1_{NLSma} (10), generating pHIV-PR_{WT}^{CFP} and pHIV-PR_{WT}^{YFP} (where WT indicates wild type), respectively.

FRET procedure. COS7 cells plated on an EZVIEW glass-bottom culture plate (Iwaki, Tokyo, Japan) were cotransfected with pHIV-PR_{WT}^{CFP} and pHIV-PR_{WT}^{YFP} using Lipofectamine 2000 (Invitrogen), according to the manufacturer's instructions, in the presence of various concentrations of each test compound, cultured for 72 h, and analyzed under a Fluoview FV500 confocal laser scanning microscope (Olympus Optical Corp., Tokyo, Japan) at room temperature, as previously described (18). In the assay, each test compound was added to the culture, followed by cotransfection. The results were determined by measurement of the quenching of the CFP (donor) fluorescence and the increase in the YFP (acceptor) fluorescence (sensitized emission), since a part of CFP energy is transferred to YFP instead of being emitted. This phenomenon can be measured by bleaching YFP, which should result in an increase in CFP fluorescence (2, 3, 27, 29). The changes in the CFP and YFP fluorescence intensities in the images of the selected regions were examined and quantified by using the FV500 image software system (Olympus Optical Corp.). The ratios of the intensities of the CFP fluorescence after photobleaching to the CFP fluorescence before photobleaching ($CFP^{A/B}$ ratios) were determined. When the $CFP^{A/B}$ ratios were <1, it was indicated that the association of the two subunits did not occur, being interpreted that protease dimerization was inhibited.

Generation of PI-resistant HIV-1 using HIV-1_{NL4-3} *in vitro*. In the experiments of the selection of drug-resistant variants, MT-4 cells were exploited as target cells, since HIV-1 in general replicates at greater levels in MT-4 cells than in MT-2 cells. MT-4 cells (10^5/ml) were exposed to HIV-1_{NL4-3} (500 $TCID_{50}$s) and cultured in the presence of various PIs at an initial concentration of an EC_{50}. Viral replication was monitored with the determination of the amount of p24 Gag produced by MT-4 cells. The culture supernatants were harvested on day 7 or by up to day 14 when the amount of p24 Gag was >250 ng/ml and used to infect fresh MT-4 cells for the next round of culture in the presence of increasing concentrations of each drug. When the virus began to propagate in the presence of the drug, the drug concentration of the following round of culture was generally increased 2- to 3-fold. To determine whether amino acid substitutions associated with HIV-1 acquisition of drug resistance occurred, high-molecular-weight DNA obtained from the lysates of the cells was subjected to nucleotide sequencing.

Generation of highly GRL-1388- and -1398-resistant HIV-1 variants using a mixture of $_{CL}$HIV-1_{MDR} isolates *in vitro*. Ten $_{CL}$HIV-1_{MDR} strains ($_{CL}$HIV-$1_{MDR/A}$, $_{CL}$HIV-$1_{MDR/B}$, $_{CL}$HIV-$1_{MDR/C}$, $_{CL}$HIV-$1_{MDR/EV}$, $_{CL}$HIV-$1_{MDR/G}$, $_{CL}$HIV-$1_{MDR/TM}$, $_{CL}$HIV-$1_{MDR/MM}$, $_{CL}$HIV-$1_{MDR/JSL}$, $_{CL}$HIV-$1_{MDR/SS}$, and $_{CL}$HIV-$1_{MDR/13-52}$) were isolated from patients with AIDS who had failed existing anti-HIV regimens after receiving 9 to 12 anti-HIV-1 drugs, not including DRV (17, 30). These strains contained 9 to 21 amino acid substitutions in protease, which have reportedly been associated with HIV-1 resistance to various PIs. The mixture of the viruses was propagated initially in MT-4 cells and PHA-PBMCs as previously described (37). The mixture was transferred to the culture with fresh MT-4 cells on day 7, and the culture supernatant was harvested and used to infect fresh MT-4 cells to continue the selection. This cycle of cell-free transmission was repeated every 7 to 14 days, each time increasing the drug concentration by a factor of 2 or 3.

Determination of nucleotide sequences. Molecular cloning and the determination of nucleotide sequences of HIV-1 passaged in the presence of each agent were performed as previously described (36, 37). In brief, high-molecular-weight DNA was extracted from HIV-1-infected MT-4 cells by using the InstaGene matrix (Bio-Rad Laboratories, Hercules, CA) and was subjected to molecular cloning, followed by sequence determination. The primers used for the first-round PCR amplification of the entire Gag- and protease-encoding regions of the HIV-1 genome were LTR F1 (5′-GAT GCT ACA TAT AAG CAG CTG C-3′) and PR12 (5′-CTC GTG ACA AAT TTC TAC TAA TGC-3′). The first-round PCR mixture consisted of 1 μl of proviral DNA solution, 2.0 U of premix *Taq* (Ex Taq version; Takara Bio, Inc., Otsu, Japan), and 12.5 pmol of each of the first-round PCR primers in a total volume of 50 μl. The PCR conditions used were an initial 2-min step at 94°C, followed by 30 cycles of 30 s at 94°C, 30 s at 58°C, and 3 min at 72°C, with a final 8 min of extension at 72°C. The first-round PCR products (1 μl) were used directly in the second round of PCR with primers LTR F2 (5′-GAG ACT CTG GTA ACT AGA GAT C-3′) and Ksma2.1 (5′-CCA TCC CGG GCT TTA ATT TTA CTG GTA C-3′) under the same PCR conditions described above. The second-round PCR products were purified with spin columns (MicroSpin S-400 HR; Amersham Biosciences Corp., Piscataway, NJ), cloned, and subjected to sequencing with a model 377 automated DNA sequencer (Applied Biosystems, Foster City, CA).

Determination of replication kinetics of GRL-1398-resistant HIV-1 variants and HIV-1_{NL4-3}. We determined the replication kinetics of two HIV-1 variant populations, which were selected in the presence of up to 1 μM GRL-1398. One population was selected for 53 weeks in experiment I (designated HIV-$1_{GRL1398\text{-}1\mu M^{Exp.I}}$) and the other for 57 weeks in experiment II (HIV-$1_{GRL1398\text{-}1\mu M^{Exp.II}}$) (see Fig. 4). MT-4 cells (3×10^5) were exposed to an HIV-

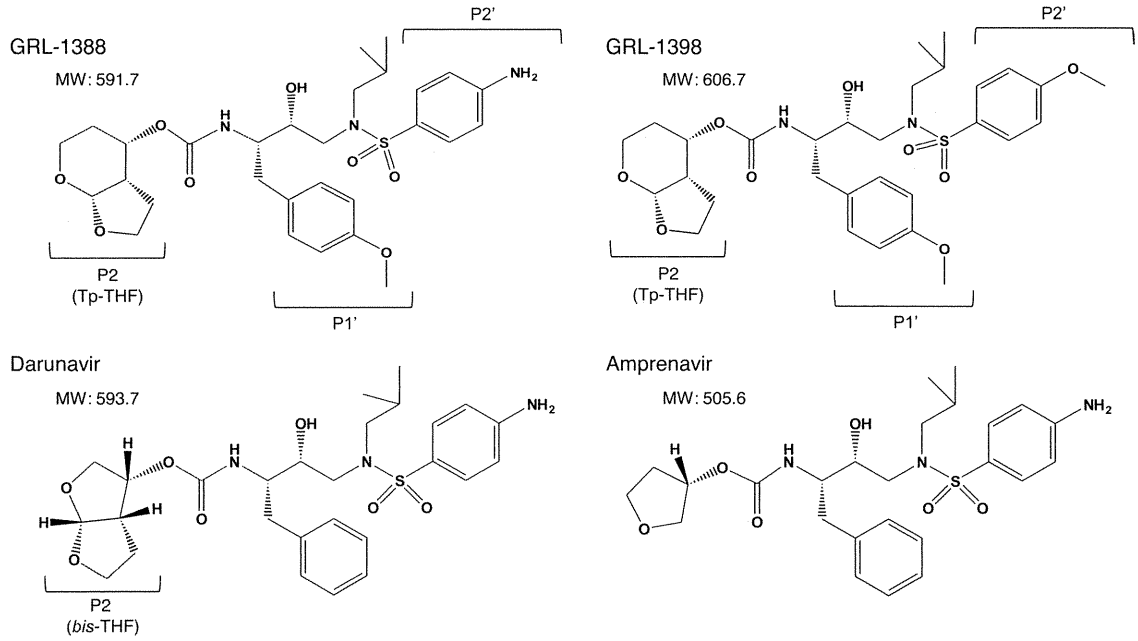

FIG. 1. Structures of GRL-1388, GRL-1398, darunavir, and amprenavir.

$1_{GRL1398\text{-}1\mu M^{Exp.I}}$, HIV-$1_{GRL1398\text{-}1\mu M^{Exp.II}}$ or wild-type HIV-$1_{NL4\text{-}3}$ preparation that contained 30 ng of p24 in six-well culture plates for 3 h, and each MT-4 cell population was divided into three fractions. Each fraction was propagated in the presence of 0, 0.1, or 1 μM GRL-1398. The amounts of p24 were measured every 2 days in culture for up to 8 or 10 days.

Modeling and analysis of GRL-1388 and -1398 interactions with wild-type HIV-1 protease. The structures of GRL-1388 and -1398 were modeled into the active site cavity of the wild-type HIV-1 protease using the extra precision Glide 5.5-ligand docking method from the Schrödinger suite of programs (8, 9, 26). Crystal structures of protease complexed with DRV (PDB code 2IEN [31]) and protease complexed with brecanavir (PDB code 2FDE [23]) obtained from the RCSB Protein Data Bank (http://www.rcsb.org) were used as template protease structures. All of the ions and glycerol-related atoms were deleted from the structures. The hydrogen atoms in both structures, 2IEN and 2FDE, were energy minimized (MacroModel, version 9.7) by using constraints on the heavy atoms of the structures. Crystallographic waters were deleted from both of the minimized structures (except the conserved water molecule that forms a tetracoordinated hydrogen bond interaction between the protease flaps and the inhibitor). These structures were then processed using the protein preparation wizard of MAESTRO (version 9.1), and the resultant structures were used to generate the receptor grid. Molecular models for GRL-1388 and -1398 were prepared by using the structure of DRV as a template. The correct stereochemistries of GRL-1388 and -1398 were assigned, and a set of diverse conformers was generated for the latter compound by using ConfGen (version 2.1). These conformers were then docked against the receptor grid. Among the docked conformers, the best binding conformations and the interactions with wild-type HIV-1 protease were analyzed. The structural model for GRL-1388 was generated by energy minimization from the optimized model of GRL-1398. Hydrogen bonds were calculated by using MAESTRO (with a 3.0-Å distance cutoff and angle constraints of 90° [donor] and 60° [acceptor], respectively), and the hydrophobic contacts of the inhibitor were obtained by probing all of the protease atoms within a radius of 4 Å using the CCP4 suite of programs (4). The programs MacroModel (version 9.7), ConfGen (version 2.1), and Glide (version 5.5) from Schrödinger LLC (New York, NY) were used in generating the final models described above. All of the graphics were prepared by using PyMOL molecular graphics program (version 0.99 DeLano Scientific LLC: http://pymol.org/).

RESULTS

Antiviral activity of GRL-1388 and -1398 against HIV-1_{LAI}. We designed and synthesized ~100 novel PIs containing the *bis*-THF component, which we reported plays a major role in the potent antiviral activity of DRV (15, 19) and its related moieties, including polycyclic ligands (11–14). Among such novel PIs, we identified GRL-1388 and -1398 (Fig. 1) as potent anti-HIV-1 agents, which contain Tp-THF. As shown in Table 1, GRL-1388 and -1398 were highly potent *in vitro* against a laboratory wild-type HIV-1 strain, HIV-1_{LAI}, with EC_{50}s of 3.6 ± 1.8 and 0.2 ± 0.2 nM, respectively, as examined in the MTT assay with $CD4^+$ MT-2 cells. Of note, the antiviral activity of GRL-1388 against HIV-1_{LAI} was comparable to or more potent than four representative U.S. Food and Drug Administration (FDA)-approved PIs: SQV, APV, ATV, and DRV. GRL-1398 was significantly more potent against HIV-1_{LAI} than these four PIs by a factor of 16.5 to 98. Both GRL-1388 and -1398 had favorable cytotoxicity profiles with 50% cytotoxicity concentrations [CC_{50}s] of more than 100 and 37.7 μM, giving selectivity index (SI) values of more than 27,800 and 188,500, respectively (Table 1).

TABLE 1. Antiviral activities of GRL-1388 and -1398 against HIV-1_{LAI} and their cytotoxicities *in vitro*[a]

Drug	Mean ± SD		Selectivity index[b]
	EC_{50} (nM)	CC_{50} (μM)	
SQV	6.2 ± 1.9	19.7 ± 6.1	3,200
APV	19.6 ± 3.9	>100	>5,100
ATV	5.0 ± 1.9	27.6 ± 0.7	5,500
DRV	3.3 ± 0.9	>100	>30,300
GRL-1388	3.6 ± 1.8	>100	>27,800
GRL-1398	0.2 ± 0.2	37.7 ± 2.7	188,500

[a] All assays were conducted in duplicate, and the data shown represent mean values (±1 standard deviation) derived from the results of three independent experiments.

[b] Each selectivity index denotes a ratio of CC_{50} to EC_{50} against HIV-1_{LAI}.

GRL-1388 and -1398 are potent against various PI-selected laboratory HIV-1 variants. We also examined whether GRL-1388 and -1398 were active against a variety of HIV-1 variants that had been selected *in vitro* with each of six FDA-approved PIs: SQV, RTV, NFV, LPV, ATV, and APV (Table 2). Each HIV-1 variant was selected *in vitro* by propagating HIV-1_{NL4-3} in the presence of increasing concentrations of each PI (up to 5 μM) in MT-4 cells and was confirmed to have acquired multiple amino acid substitutions in protease of the virus, which have reportedly been associated with viral resistance to PIs (see footnote *a* of Table 2). Each of the variants (HIV-$1_{SQV\text{-}5\mu M}$, HIV-$1_{RTV\text{-}5\mu M}$, HIV-$1_{NFV\text{-}5\mu M}$, HIV-$1_{LPV\text{-}5\mu M}$, and HIV-$1_{ATV\text{-}5\mu M}$) was highly resistant to the corresponding PI, with which the variant was selected, having the EC_{50}s of >1 μM, and the fold differences in the EC_{50}s relative to the EC_{50} of each drug against HIV-1_{NL4-3} ranged from >25 to >400 (Table 2). The activity of GRL-1388 against all five variants was well maintained, with the fold changes being 1 to 11. GRL-1398 was significantly more potent against five such HIV-1 variants than DRV with an EC_{50} of 0.1 to 5.7 nM. Of note, GRL-1388 and -1398 were moderately active against HIV-$1_{APV\text{-}5\mu M}$, with EC_{50}s of 475.7 and 49.0 nM, presumably due to the structural resemblance of GRL-1388 and -1398 to APV (Fig. 1).

GRL-1388 and -1398 exert potent activity against multiple-PI-resistant clinical HIV-1 strains ($_{CL}$HIV-1_{MDR}). We also sought to determine whether GRL-1388 and -1398 were active against $_{CL}$HIV-1_{MDR} isolates, including $_{CL}$HIV-$1_{MDR/B}$, $_{CL}$HIV-$1_{MDR/C}$, $_{CL}$HIV-$1_{MDR/G}$, $_{CL}$HIV-$1_{MDR/TM}$, $_{CL}$HIV-$1_{MDR/MM}$, and $_{CL}$HIV-$1_{MDR/JSL}$, which contained 9 to 14 PI-resistance-associated amino acid substitutions in protease (see footnote *a* of Table 3). The EC_{50}s of LPV against these multi-PI-resistant clinical HIV-1 isolates were mostly >1 μM, and the activity of other three PIs (SQV, ATV, and APV) had also been significantly compromised, as determined using PHA-PBMCs as the target cells and p24 production inhibition as the endpoint (Table 3). Both GRL-1388 and DRV remained active against all of the clinical variants examined and the fold differences between the EC_{50}s against HIV-$1_{ERS104pre}$ and those against each clinical variant ranged from as low as 1 to 7. The fold changes seen with GRL-1398 ranged from 1 to 16; however, the absolute EC_{50}s remained substantially lower, ranging from 0.3 to 4.8 nM, than those of DRV (Fig. 2).

GRL-1398 is active against DRV-resistant variants. We determined antiviral activity against DRV-resistant HIV-1 variants that had been selected *in vitro* by propagating a mixture of eight $_{CL}$HIV-1_{MDR} strains in the presence of increasing concentrations of DRV in MT-4 cells (17). Two such variants, HIV-1_{DRV^RP10} and HIV-1_{DRV^RP20}, containing a set of amino acid substitutions at passages 10 and 20, respectively (Table 4), were resistant to DRV with EC_{50}s of 29.1 and 214.1 nM and to GRL-1388 with EC_{50}s of 24.6 and 150.8 nM. In contrast, GRL-1398 had substantially lower absolute EC_{50}s—3.3 and 21.9 nM against HIV-1_{DRV^RP10} and HIV-1_{DRV^RP20}, respectively(Table 4).

GRL-1388 and -1398 moderately disrupt the dimerization of HIV-1 protease. We previously reported that DRV effectively disrupts the dimerization of HIV-1 protease monomer subunits as determined with the FRET/HIV-1 expression assay (18). We therefore sought to determine whether GRL-1388

TABLE 2. Antiviral activities of GRL-1388 and -1398 against laboratory PI-selected HIV-1variants[a]

Virus	Mean EC_{50} in nM ± SD (fold change)								
	SQV	RTV	NFV	LPV	ATV	APV	DRV	GRL-1388	GRL-1398
HIV-1_{NL4-3}	5.2 ± 1.7	40.4 ± 4.9	30.2 ± 3.0	27.8 ± 5.3	2.5 ± 0.8	34.3 ± 1.3	3.2 ± 0.3	3.1 ± 0.2	0.2 ± 0.1
HIV-$1_{SQV\text{-}5\mu M}$	>1,000 (192)	>1,000 (>25)	>1,000 (>33)	>1,000 (>36)	415.0 ± 15.1 (166)	353.7 ± 12.4 (10)	30.4 ± 0.5 (10)	32.6 ± 7.5 (11)	5.7 ± 1.3 (29)
HIV-$1_{RTV\text{-}5\mu M}$	66.3 ± 8.9 (13)	>1,000 (>25)	386.4 ± 84.7 (13)	698.3 ± 87.4 (25)	32.5 ± 5.9 (13)	334.5 ± 42.5 (10)	19.9 ± 13.5 (6)	28.8 ± 1.8 (9)	3.1 ± 0.2 (16)
HIV-$1_{NFV\text{-}5\mu M}$	24.1 ± 6.3 (5)	46.5 ± 9.4 (1)	>1,000 (>33)	37.2 ± 3.3 (1)	12.3 ± 2.2 (5)	71.3 ± 10.5 (2)	2.7 ± 0.4 (1)	2.6 ± 0.4 (1)	0.1 ± 0.1 (1)
HIV-$1_{LPV\text{-}5\mu M}$	33.5 ± 0.9 (6)	>1,000 (>25)	401.6 ± 11.0 (13)	>1,000 (>36)	17.0 ± 7.7 (7)	320.7 ± 23.2 (9)	4.0 ± 0.9 (1)	29.9 ± 12.5 (10)	3.5 ± 0.4 (18)
HIV-$1_{ATV\text{-}5\mu M}$	134.3 ± 22.8 (26)	>1,000 (>25)	>1,000 (>33)	>1,000 (>36)	>1,000 (>400)	521.0 ± 124.1 (15)	6.8 ± 0.6 (2)	21.9 ± 7.7 (7)	3.1 ± 0.4 (16)
HIV-$1_{APV\text{-}5\mu M}$	47.3 ± 2.1 (9)	>1,000 (>25)	>1,000 (>33)	633.2 ± 21.0 (23)	453.6 ± 12.2 (181)	>1,000 (>29)	423.9 ± 6.0 (132)	475.7 ± 38.1 (153)	49.0 ± 1.1 (245)

[a] The amino acid substitutions identified in protease of HIV-$1_{SQV\text{-}5\mu M}$, HIV-$1_{RTV\text{-}5\mu M}$, HIV-$1_{NFV\text{-}5\mu M}$, HIV-$1_{LPV\text{-}5\mu M}$, HIV-$1_{ATV\text{-}5\mu M}$, and HIV-$1_{APV\text{-}5\mu M}$ compared to the consensus type B sequence cited from the Los Alamos database include L10I/N37D/G48V/I54V/L63P/G73C/I84V/L90M, L10I/M46L/I54V/V82A, L10F/K20T/D30N/K45I/A71V/V77I, L10F/M46I/I54V/V82A, L23I/E34Q/K43I/M46I/I50L/G51A/L63P/A71V/V82A/T91A, and L10F/V32I/L33F/M46L/I54M/A71V, respectively. Numbers in parentheses represent fold changes in EC_{50}s for each isolate compared to the EC_{50}s for wild-type HIV-1_{NL4-3}. All assays were conducted in duplicate or triplicate, and the data shown represent mean values (±1 standard deviation) derived from the results of three independent experiments.

TABLE 3. Antiviral activity of GRL-1388 and -1398 against multidrug-resistant clinical isolates in PHA-PBMCs[a]

Virus (syncytium formation)	Mean EC_{50} in nM ± SD (fold change)						
	SQV	LPV	ATV	APV	DRV	GRL-1388	GRL-1398
$_{CL}$HIV-$1_{ERS104pre}$ (SI)	4.4 ± 1.8	41.0 ± 6.0	1.9 ± 1.2	35.1 ± 4.3	3.5 ± 0.6	3.2 ± 0.3	0.3 ± 0.1
$_{CL}$HIV-$1_{MDR/B}$ (SI)	206.9 ± 81.2 (47)	>1,000 (>24)	228.0 ± 82.6 (120)	328.8 ± 138.7 (9)	19.4 ± 3.6 (6)	4.7 ± 3.6 (1)	4.8 ± 0.3 (16)
$_{CL}$HIV-$1_{MDR/C}$ (SI)	38.8 ± 16.2 (9)	>1,000 (>24)	25.4 ± 7.5 (13)	265.2 ± 79.8 (8)	5.2 ± 1.5 (1)	4.0 ± 1.0 (1)	1.1 ± 0.1 (4)
$_{CL}$HIV-$1_{MDR/G}$ (SI)	26.3 ± 2.4 (6)	319.3 ± 31.0 (8)	16.3 ± 4.5 (9)	260.1 ± 55.8 (7)	5.1 ± 2.3 (1)	6.2 ± 0.6 (2)	1.6 ± 1.1 (5)
$_{CL}$HIV-$1_{MDR/TM}$ (SI)	110.6 ± 48.6 (25)	658.1 ± 115.9 (16)	22.4 ± 3.8 (12)	197.7 ± 65.0 (6)	3.7 ± 1.3 (1)	2.7 ± 0.7 (1)	0.3 ± 0.1 (1)
$_{CL}$HIV-$1_{MDR/MM}$ (NSI)	190.7 ± 75.9 (43)	>1,000 (>24)	68.9 ± 27.8 (36)	402.2 ± 193.9 (11)	21.4 ± 1.7 (6)	21.3 ± 5.0 (7)	2.6 ± 1.4 (9)
$_{CL}$HIV-$1_{MDR/JSL}$ (NSI)	281.8 ± 35.7 (64)	>1,000 (>24)	347.0 ± 56.9 (183)	306.6 ± 124.4 (9)	16.0 ± 4.4 (5)	18.8 ± 9.0 (6)	3.1 ± 0.1 (10)

[a] Amino acid substitutions identified in protease compared to the consensus type B sequence cited from the Los Alamos database include L63P in $_{CL}$HIV-$1_{ERS104pre}$; L10I, K14R, L33I, M36I, M46I, F53I, K55R, I62V, L63P, A71V, G73S, V82A, L90M, and I93L in $_{CL}$HIV-$1_{MDR/B}$; L10I, I15V, K20R, L24I, M36I, M46L, I54V, I62V, L63P, K70Q, V82A, and L89M in $_{CL}$HIV-$1_{MDR/C}$; L10I, V11I, T12E, I15V, L19I, R41K, M46L, L63P, A71T, V82A, and L90M in $_{CL}$HIV-$1_{MDR/G}$; L10I, K14R, R41K, M46L, I54V, L63P, A71V, V82A, L90M, and I93L in $_{CL}$HIV-$1_{MDR/TM}$; L10I, K43T, M46L, I54V, L63P, A71V, V82A, L90M, and Q92K in $_{CL}$HIV-$1_{MDR/MM}$; L10I, L24I, I33F, E35D, M36I, N37S, M46L, I54V, R57K, I62V, L63P, A71V, G73S, and V82A in $_{CL}$HIV-$1_{MDR/JSL}$. $_{CL}$HIV-$1_{ERS104pre}$ served as a source of wild-type HIV-1. Numbers in parentheses represent the fold changes of EC_{50}s against each isolate compared to the EC_{50}s against wild-type $_{CL}$HIV-$1_{ERS104pre}$. All assays were conducted in duplicate or triplicate, and the data shown represent mean values (±1 standard deviation) derived from results of three independent experiments. PHA-PBMCs were derived from a single donor in each experiment.

and -1398 exerted such protease dimerization inhibition activity. In the absence of agents, the mean $CFP^{A/B}$ ratio obtained in the assay was 1.12, indicating that protease dimerization clearly occurred (Fig. 3). However, when COS7 cells were cotransfected in the presence of 1 μM GRL-1388 and -1398, protease dimerization still occurred, with the mean $CFP^{A/B}$ ratios being 1.02 and 1.10, respectively. However, the mean $CFP^{A/B}$ ratios obtained in the presence of 10 and 20 μM GRL-1388 and -1398 were all <1.0, indicating that both compounds blocked the dimerization. Of note, DRV blocked the dimerization at as low as 1.0 μM under the same conditions, suggesting that GRL-1388 and -1398 had relatively moderate activity to disrupt the dimerization of HIV-1 protease compared to DRV.

***In vitro* selection of HIV-1 variants resistant to GRL-1388 and -1398.** We attempted to select HIV-1 variants resistant to GRL-1388 and -1398 by propagating $HIV\text{-}1_{NL4\text{-}3}$ in MT-4 cells in the presence of increasing concentrations of each compound. Considering that drug resistance-associated amino acid substitutions occur stoichiometrically at random, we conducted the selection with GRL-1398 on two different occasions. When selected in the presence of increasing concentrations of RTV and APV, the virus quickly became resistant to the drugs and started replicating in the presence of 5 μM at 18 and 26 weeks of selection (Fig. 4) and had acquired L10I/M46L/I54V/V82A and L10F/V32I/L33F/M46L/I54M/A71V, respectively (Fig. 4). In contrast, the acquisition of resistance to GRL-1398 was significantly delayed and it took 53 and 57 weeks in the selection until the virus started replicating in the presence of 1 μM in experiments I and II, respectively (Fig. 4). The virus preparations selected with GRL-1398 in experiments I and II had acquired no amino acid substitutions in protease by 20 and 16 weeks of culture; however, they acquired apparently resistance-associated substitutions by 26 and 22 weeks with L10F/M46I/I50V and L10F, respectively. The virus had acquired A28S by 28 weeks of culture, along with L10F and M46M/I in experiment II ($HIV_{1398^{II\text{-}Wk28}}$); thereafter, $HIV_{1398^{II\text{-}Wk28}}$ appeared to start developing resistance at a faster rate, although the virus in experiment I did not acquire A28S but had L10F/M46I/I50V and developed resistance. In contrast, when $HIV\text{-}1_{NL4\text{-}3}$ was selected with GRL-1388 under the same conditions, the virus remained wild-type over 45 weeks of selection, whereas $HIV\text{-}1_{NL4\text{-}3}$, selected with DRV, had acquired V82I by 14 weeks. All amino acid substitutions identified during the selection are illustrated in Fig. S1 in the supplemental material.

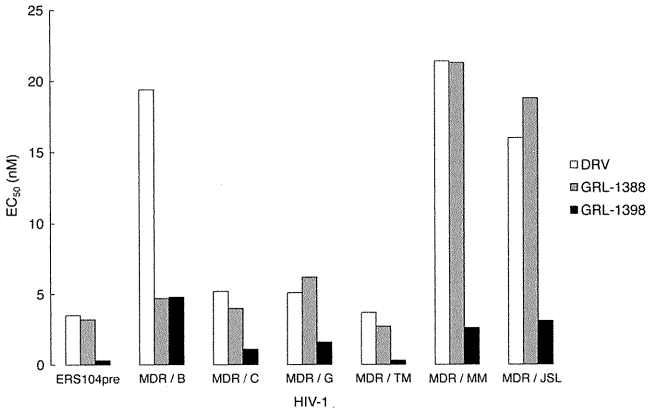

FIG. 2. Antiviral activity of GRL-1388, GRL-1398, and darunavir against multidrug-resistant clinical HIV-1 isolates. The EC_{50}s of darunavir (white), GRL-1388 (gray), and GRL-1398 (black) against $_{CL}$HIV-$1_{ERS104pre}$, which served as a wild-type HIV-1, and six $_{CL}$HIV-1_{MDR} isolates were determined as described in the legend to Table 3 and Materials and Methods. Note that the EC_{50}s of GRL-1398 against all of these isolates were substantially lower than those of DRV.

Selection with GRL-1388 and -1398 of a mixture of 10 $_{CL}$HIV-1_{MDR} variants. Considering that amino acid substitutions in HIV-1 stoichiometrically and randomly occur and the resulting amino acid substitutions can vary from one experiment to another as seen above (Fig. 4), we performed an additional selection experiment with MT4 cells and a mixture of 10 $_{CL}$HIV-1_{MDR} variants as a starting virus population with DRV, GRL-1388, and -1398. In line with our previous observations that a highly DRV-resistant HIV-1 variants emerged when selected with DRV using a mixture of eight $_{CL}$HIV-1_{MDR} variants (17), HIV-1 started replicating in the presence of 5 μM DRV and GRL-1388 by 21 and 17 weeks of selection, respectively (Fig. 5). In contrast to the results of selection experiments using MT-4 cells and $HIV\text{-}1_{NL4\text{-}3}$, in which HIV-1 started replicating with GRL-1398, but not with GRL-1388 or DRV (Fig. 4), the emergence of HIV-1 capable of replicating

TABLE 4. Antiviral activity of GRL-1388 and -1398 against laboratory darunavir-resistant HIV-1[a]

Virus	Amino acid substitution(s) in protease	Mean EC_{50} in nM ± SD (fold change)		
		DRV	GRL-1388	GRL-1398
$cHIV\text{-}1_{ERS104pre}$	L63P	4.0 ± 1.0	2.5 ± 0.4	0.4 ± 0.1
$HIV\text{-}1_{DRV^{R}P10}$	L10I, I15V, K20R, L24I, V32I, M36I, M46L, I54V, I62V, L63P, K70Q, V82A, L88M	29.1 ± 0.9 (7)	24.6 ± 6.9 (10)	3.3 ± 0.3 (8)
$HIV\text{-}1_{DRV^{R}P20}$	L10I, I15V, K20R, L24I, V32I, M36I, M46L, L63P, A71T, V82A, L88M	214.1 ± 47.9 (54)	150.8 ± 46.7 (60)	21.9 ± 5.7 (54)

[a] DRV-resistant HIV-1 variants were selected *in vitro* by propagating a mixture of eight $_{CL}HIV\text{-}1_{MDR}$ isolates in the presence of increasing concentrations of DRV in MT-4 cells. Six of the eight isolates were the same as those used for drug susceptibility assay (Table 3). Amino acid substitutions identified in protease of the other two isolates compared to the consensus type B sequence cited from the Los Alamos database include L10I, I15V, E35D, N37E, K45R, I54V, L63P, A71V, V82T, L90M, I93L, and C95F in $_{CL}HIV\text{-}1_{MDR/A}$ and L10R, N37D, M46I, I62V, L63P, A71V, G73S, V74I, V82T, L90M, and I93L in $_{CL}HIV\text{-}1_{MDR/SS}$. Numbers in parentheses represent the fold changes of EC_{50}s against each isolate compared to the EC_{50}s against $HIV\text{-}1_{ERS104pre}$. All assays were conducted in duplicate or triplicate, and the data shown represent mean values (±1 standard deviation) derived from the results of three independent experiments. PHA-PBMCs were derived from a single donor.

in the presence of GRL-1398 was significantly delayed compared to the cases with GRL-1388 and DRV (Fig. 5). Sequence analyses of the protease-encoding gene of the viruses in these selection experiments revealed that the HIV-1 replicating in the presence of GRL-1398 had acquired A28S by 24 weeks of selection (see Fig. S2 in the supplemental material), when the virus appeared to obtain robust replication fitness despite the presence of GRL-1398. There was no A28S substitution in those selected with GRL-1388 or DRV, as seen in the selection experiments discussed above in Fig. 4. All amino acid substitutions identified during the selection are illustrated in Fig. S2 in the supplemental material.

Effects of amino acid substitutions in the protease of GRL-1398-resistant variants on the antiviral activity of GRL-1388 and DRV. We also examined whether GRL-1398-resistant variants had cross-resistance with GRL-1388 and DRV. As described above, we selected two HIV-1 variant populations in the presence of up to 1 μM GRL-1398 (Fig. 4). One population was selected for 53 weeks in experiment I (designated as $HIV\text{-}1_{GRL1398\text{-}1\mu M^{Exp.I}}$) and the other for 57 weeks in experiment II ($HIV\text{-}1_{GRL1398\text{-}1\mu M^{Exp.II}}$). These two populations were resistant to GRL-1398 with EC_{50}s of 505.1 and 552.8 nM (Table 5). GRL-1388 and DRV were moderately active against $HIV\text{-}1_{GRL1398\text{-}1\mu M^{Exp.I}}$, whereas both GRL-1388 and DRV essentially lost their activity against $HIV\text{-}1_{GRL1398\text{-}1\mu M^{Exp.II}}$, having EC_{50}s of >1,000 nM (Table 5).

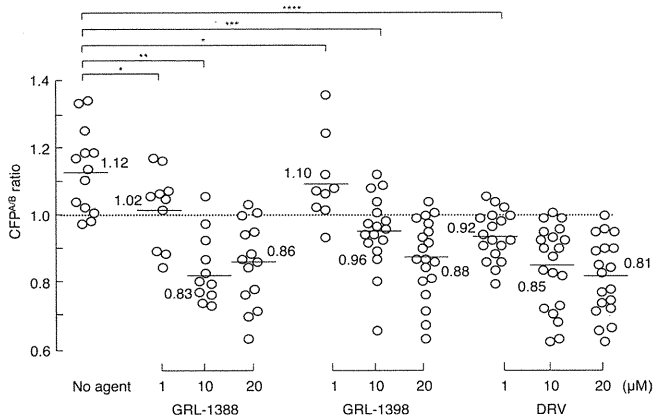

FIG. 3. Inhibition of HIV-1 protease dimerization. COS7 cells were exposed to each of the agents (GRL-1388, GRL-1398, and DRV) in various concentrations (1, 10, and 20 μM) and subsequently cotransfected with plasmids encoding full-length molecular infectious HIV-1 ($HIV_{NL4\text{-}3}$) clones producing CFP- or YFP-tagged protease. After 72 h, cultured cells were examined in the FRET-based HIV-1 expression assay and the $CFP^{A/B}$ ratios (*y* axis) were determined. The mean values of the ratios obtained are shown as horizontal bars. A $CFP^{A/B}$ ratio that is >1 signifies that protease dimerization occurred, whereas a ratio that is <1 signifies the disruption of protease dimerization. All of the experiments were conducted in a blind fashion. *, Not significant; **, $P < 0.0001$; ***, $P = 0.0005$; ****, $P = 0.0001$.

Moderately compromised replication fitness of GRL-1398-resistant HIV-1 variants. We have conducted a replication kinetics assay and determined the fitness of $HIV\text{-}1_{GRL1398\text{-}1\mu M^{Exp.I}}$, $HIV\text{-}1_{GRL1398\text{-}1\mu M^{Exp.II}}$, and $HIV\text{-}1_{NL4\text{-}3}$ with or without GRL-1398 (0, 0.1, 1 μM). It is of note that the resistant viruses were selected and adapted in MT-4 cells, and MT-4 cells were used in the assay. Although $HIV\text{-}1_{NL4\text{-}3}$ failed to replicate in the presence of 0.1 and 1 μM GRL-1398, both $HIV\text{-}1_{GRL1398\text{-}1\mu M^{Exp.I}}$ and $HIV\text{-}1_{GRL1398\text{-}1\mu M^{Exp.II}}$ replicated despite the presence of GRL-1398 (Fig. 6). It is also noteworthy that when $HIV\text{-}1_{GRL1398\text{-}1\mu M^{Exp.I}}$ and $HIV\text{-}1_{GRL1398\text{-}1\mu M^{Exp.II}}$ were propagated in the presence or absence of GRL-1398, their replication activities were found to be moderately compromised compared to that of $HIV\text{-}1_{NL4\text{-}3}$ without GRL-1398 (Fig. 6).

GRL-1398 forms greater interactions with protease than GRL-1388. Analysis of the molecular complexes of GRL-1388 and -1398 with wild-type HIV-1 protease, generated by docking simulations, revealed that GRL-1398 has a greater number of hydrophobic interactions with protease compared to GRL-1388 and DRV (Fig. 7). The bicyclic structure of Tp-THF representing the P2 group in both GRL-1388 and -1398 shows hydrogen bond interactions with the backbone amide nitrogen atoms of Asp29 and Asp30, similar to that of the *bis*-THF of DRV. The oxygen atoms of the pyran and the furan rings showed two and one hydrogen bonds with the amide nitrogen atoms of Asp29 and Asp30, respectively. The transition state mimetic hydroxyl group in both compounds shows two hydrogen bonds with the catalytic Asp25, in addition, GRL-1398 shows a hydrogen bond with the catalytic Asp25′ residue of protease. The P2′ amine group in GRL-1388 has a potential to form contacts with the delta oxygen atoms on the side chains of Asp29′ and Asp30′, respectively. The oxygen atom from the O-methoxy (P2′) functional group of GRL-1398 has a potential to form hydrogen bonds with the two backbone amide nitrogen atoms of Asp29′ and Asp30′, respectively. Both GRL-1388 and -1398 form hydrogen bonds with the conserved bridg-

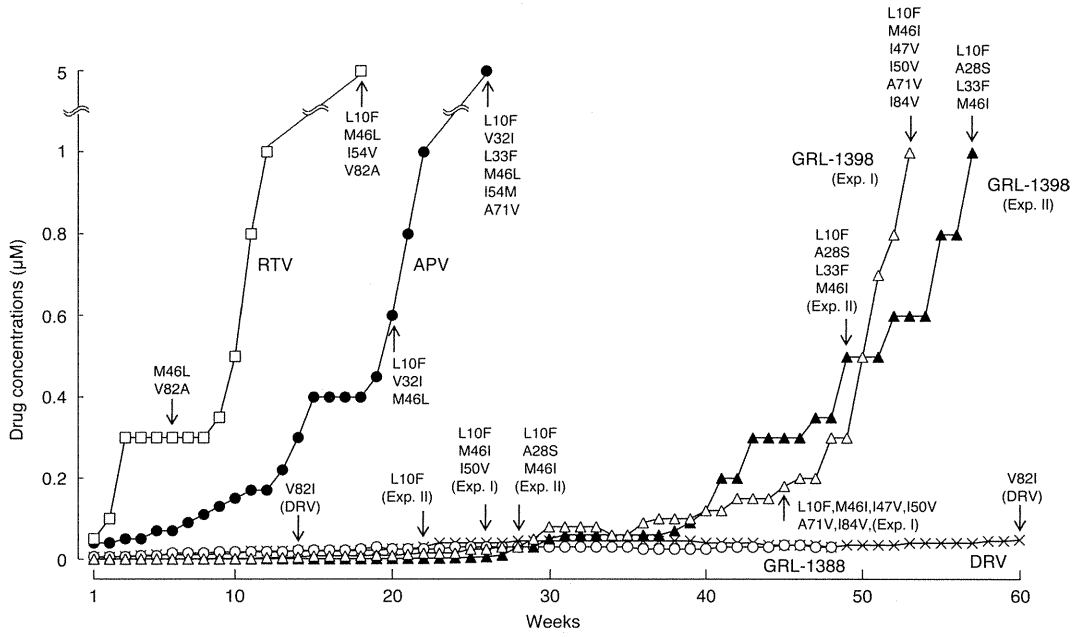

FIG. 4. *In vitro* selection of HIV-1 variants against GRL-1388 and -1398. HIV-1_{NL4-3} was propagated in MT-4 cells in the presence of increasing concentrations of ritonavir (□), amprenavir (●), darunavir (×), GRL-1388 (○), or GRL-1398 (experiment I △ and experiment II ▲). Each passage of the virus was carried out in a cell-free manner. Amino acid substitutions identified in the protease of each HIV-1 at each indicated time of the selection are shown. Note that, by week 48, no amino acid mutations were detected in the protease of GRL-1388-resistant isolate. All amino acid substitutions identified during the selection are illustrated in Fig. S1 in the supplemental material.

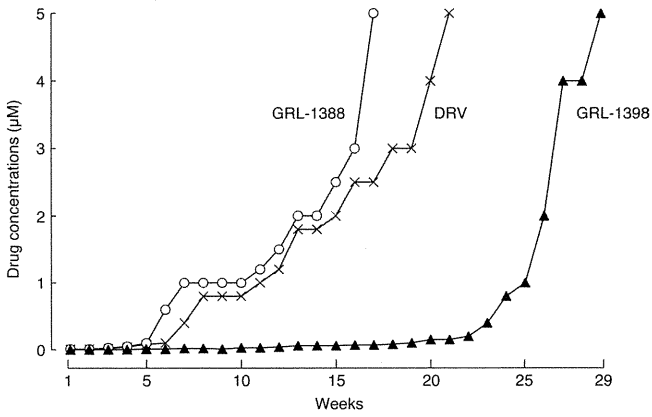

FIG. 5. *In vitro* selection multidrug-resistant clinical isolates against GRL compounds and DRV. A mixture of 10 $_{CL}$HIV-1_{MDR} variants were propagated in MT-4 cells in the presence of increasing concentrations of darunavir (×), GRL-1388 (○), or GRL-1398 (▲). Each selection was conducted in a cell-free fashion. The amino acid substitutions in protease of eight $_{CL}$HIV-1_{MDR} isolates are given in the footnotes for Tables 3 and 4. The amino acid substitutions identified in protease were L10V, T12E, G16A, L19I, K20R, L33F, E35D, M36I, N37S, M46I, I50V, F53L, I54V, K55R, R57K, D60E, I62V, L63P, A71V, V82A, and L90M in $_{CL}$HIV-$1_{MDR/EV}$ and N47D, I54V, D60E, L63P, A71V, V74I, V82A, L90M, and I93L in $_{CL}$HIV-$1_{MDR/13-52}$. HIV-1 strains, capable of replicating in the presence of each agent at 5 μM, had acquired L10V, T12E, G16A, L19I, K20R, V32I, L33F, E34K, E35D, M36I, N37S, M46I, I50V, F53L, I54V, K55R, R57K, D60E, I62V, L63P, A71V, G73S,V82A, and L90M in $HIV_{MIX\text{-}DRV}^{WK21}$; L10V, T12E, G16A, L19I, K20R, V32I, L33F, E35D, M36I, N37S, M46I, I50V, F53L, I54V, K55R, R57K, D60E, I62V, L63P, A71V, V82A, and L90M in $HIV_{MIX\text{-}1388}^{WK17}$; and L10I, I15V, A28S, L33I, M36I, M46I, I50V, F53L, K55R, I62V, L63P, A71V, G73S, L90M, and I93L in $HIV_{MIX\text{-}1398}^{WK29}$. The amino acid substitutions identified in each HIV-1 during the selection are illustrated in Fig. S2 in the supplemental material.

ing water molecule that connects to the protease flaps via hydrogen bonds with the amide nitrogen atoms of I50 and I50′. As shown in Table 6, the hydrophobic contacts were examined for both compounds and were compared to each other as well as to those of DRV. GRL-1388 has a similar interaction profile as DRV, whereas GRL-1398 has an overall greater number of interactions.

DISCUSSION

We have previously designed and synthesized a series of PIs possessing a *bis*-THF moiety that interacts with the backbone atoms of the catalytic site amino acids, Asp29 and Asp30, of HIV-1 protease (1, 19, 32). In the present study, we report two newly generated PIs, GRL-1388 and -1398 (Fig. 1), containing a polycyclic ligand, Tp-THF, in place of the *bis*-THF moiety, which displayed potent anti-HIV-1 activity against wild-type HIV-1 and a wide spectrum of laboratory and primary multi-PI-resistant HIV-1 strains with favorable cytotoxicity profiles *in vitro*. Structurally, GRL-1388 has a methoxybenzene moiety and an aminobenzene moiety at the P1′ and P2′ sites, respectively, while GRL-1398 has a methoxybenzene moiety at each of the P1′ and P2′ sites, respectively. The activity of GRL-1388 against HIV-1_{LAI} was comparable to or more potent than four representative FDA-approved PIs, SQV, APV, ATV, and DRV, whereas that of GRL-1398 was significantly more potent than these four PIs by factors of 16.5 to 98 (Table 1). It should be noted that the cytotoxicity of GRL-1398 is relatively greater, with a CC_{50} value of 37.7 μM and a SI of 188,500, compared to GRL-1388 with a CC_{50} value of >100 μM and an SI of >27,800. The mechanism of the relatively greater cytotoxicity of GRL-1398 compared to that of GRL-1388 is unknown at

TABLE 5. Antiviral activity of darunavir and GRL-1388 against GRL-1398-resistant HIV-1[a]

Virus	Amino acid substitutions in protease	Mean EC_{50} (nM) ± SD		
		DRV	GRL-1388	GRL-1398
$HIV\text{-}1_{NL4\text{-}3}$		3.1 ± 0.4	3.0 ± 0.3	0.2 ± 0.1
$HIV\text{-}1_{GRL1398\text{-}1\mu M}{}^{Exp.I}$	L10F, M46I, I47V, I50V, A71V, I84V	67.3 ± 12.0	151.9 ± 10.5	505.1 ± 168.0
$HIV\text{-}1_{GRL1398\text{-}1\mu M}{}^{Exp.II}$	L10F, A28S, L33F, M46I	>1,000	>1,000	552.8 ± 213.3

[a] GRL-1398-resistant HIV-1 was selected *in vitro* by propagating $HIV\text{-}1_{NL4\text{-}3}$ in the presence of increasing concentrations of GRL-1398 in MT-4 cells (Fig. 4). All assays to determine the EC_{50}s were conducted in duplicate or triplicate, and the data shown represent mean values (±1 standard deviation) derived from the results of three independent assays.

this time. Nevertheless, the CC_{50} values of two currently widely used FDA-approved PIs, SQV and ATV, were 19.7 and 27.6 μM, with their SI values of 3,200 and 5,500, respectively, when assessed under the same conditions together with GRL-1388 and -1398 (Table 1). Thus, even if GRL-1398 is relatively more cytotoxic than GRL-1388, one can assume that the level of toxicity of GRL-1398 is likely to be reasonably favorable, although the actual safety issue of GRL-1388 and -1398 has to be carefully examined in the setting of preclinical and clinical trials as needed.

GRL-1388 was also potently active against HIV-1 variants, which were selected to be resistant *in vitro* to each of five FDA-approved PIs, SQV, RTV, NFV, LPV, and ATV. GRL-1398 was significantly more potent against such five HIV-1variants with EC_{50}s of as low as 0.1 to 5.7 nM (Table 2). It is noteworthy that both GRL-1388 and -1398 were moderately active against $HIV\text{-}1_{APV\text{-}5\mu M}$, with EC_{50}s of 475.7 and 49.0 nM, which is explained by the fact that the two compounds have a resemblance to APV, as does DRV (Fig. 1). Moreover, GRL-1388 was also potent against all six highly multi-PI-resistant clinical HIV-1 isolates examined with the observed fold differences between EC_{50}s against a wild-type clinical isolate $HIV\text{-}1_{ERS104pre}$ and those against each clinical variant, ranging from as low as 1 to 7. The fold changes seen with GRL-1398 similarly ranged from 1 to 16; however, the absolute EC_{50}s of GRL-1398 remained substantially low, ranging from 0.3 to 4.8 nM, compared to 3.7 to 21.4 nM for DRV (Table 3 and Fig. 2). These data strongly suggest that these two new PIs could serve as good candidates for further development as potential anti-HIV-1 therapeutics, but it was noted that, of the two compounds, GRL-1398 could be more promising since it is such a potent PI against both wild-type HIV-1 and various multi-PI-resistant HIV-1 variants.

We previously demonstrated that DRV effectively disrupts the dimerization of HIV-1 protease monomer subunits, as determined with a FRET/HIV-1 expression assay (18); this might explain the reason for the highly favorable clinical efficacy and high-level genetic barrier against HIV-1 acquisition of resistance to DRV in clinical settings (6, 21, 25). However, the protease dimerization inhibition activity of both GRL-1388 and -1398 was modest compared to that of DRV, suggesting that the protease dimerization activity of GRL-1388 and -1398 does not appear to significantly contribute to the potency of the two compounds. Indeed, none or only one of the set of four amino acid substitutions (V32I, L33F, I54M, and I84V), which appears to reduce the activity of DRV to disrupt HIV-1 protease dimerization (17), was seen in the protease of HIV-1 that replicated in the presence of high concentrations of GRL-1398, although both V32I and L33F were seen in $HIV_{MIX\text{-}DRV}{}^{WK19}$ and $HIV_{MIX\text{-}DRV}{}^{WK21}$ (see Fig. S2 in the supplemental material). Of interest, when $HIV\text{-}1_{NL4\text{-}3}$ was propagated in the presence of GRL-1398, the A28S substitu-

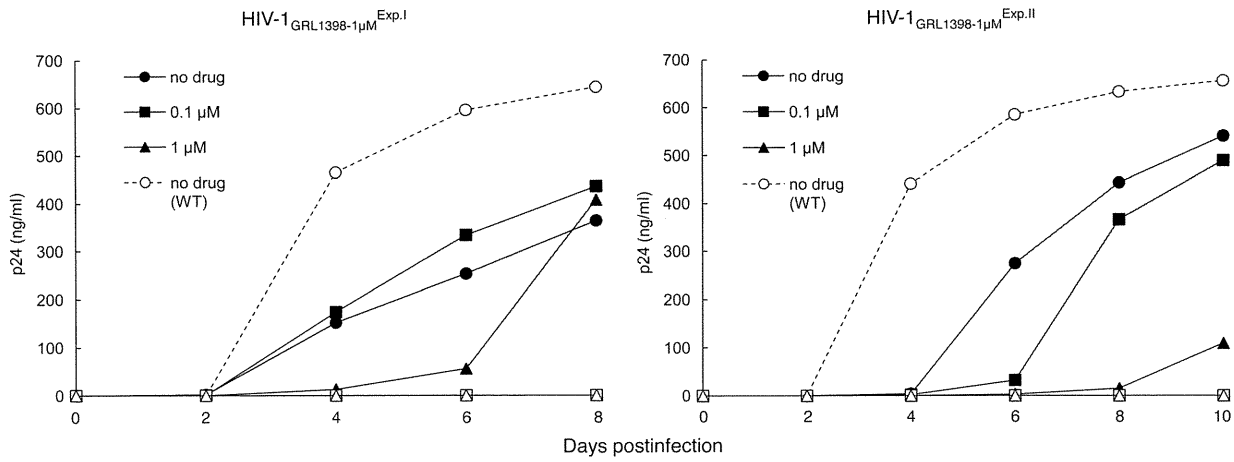

FIG. 6. Replication kinetics of GRL-1398-resistant HIV-1 variants and $HIV\text{-}1_{NL4\text{-}3}$. MT-4 cells were exposed to $HIV\text{-}1_{GRL1398\text{-}1\mu M}{}^{Exp.I}$ (left panel, closed symbols), $HIV\text{-}1_{GRL1398\text{-}1\mu M}{}^{Exp.II}$ (right panel, closed symbols), or wild-type $HIV\text{-}1_{NL4\text{-}3}$ (WT, ○) for 3 h, and each MT-4 cell population was cultured in the presence of 0.1 μM (■) or 1 μM (▲) of GRL-1398 or without the agent (●). The amounts of p24 were measured every 2 days for up to 8 or 10 days. Note that $HIV\text{-}1_{NL4\text{-}3}$ failed to replicate in the presence of 0.1 and 1 μM GRL-1398 (□ and △, respectively), both $HIV\text{-}1_{GRL1398\text{-}1\mu M}{}^{Exp.I}$ and $HIV\text{-}1_{GRL1398\text{-}1\mu M}{}^{Exp.II}$ replicated in the presence of GRL-1398.

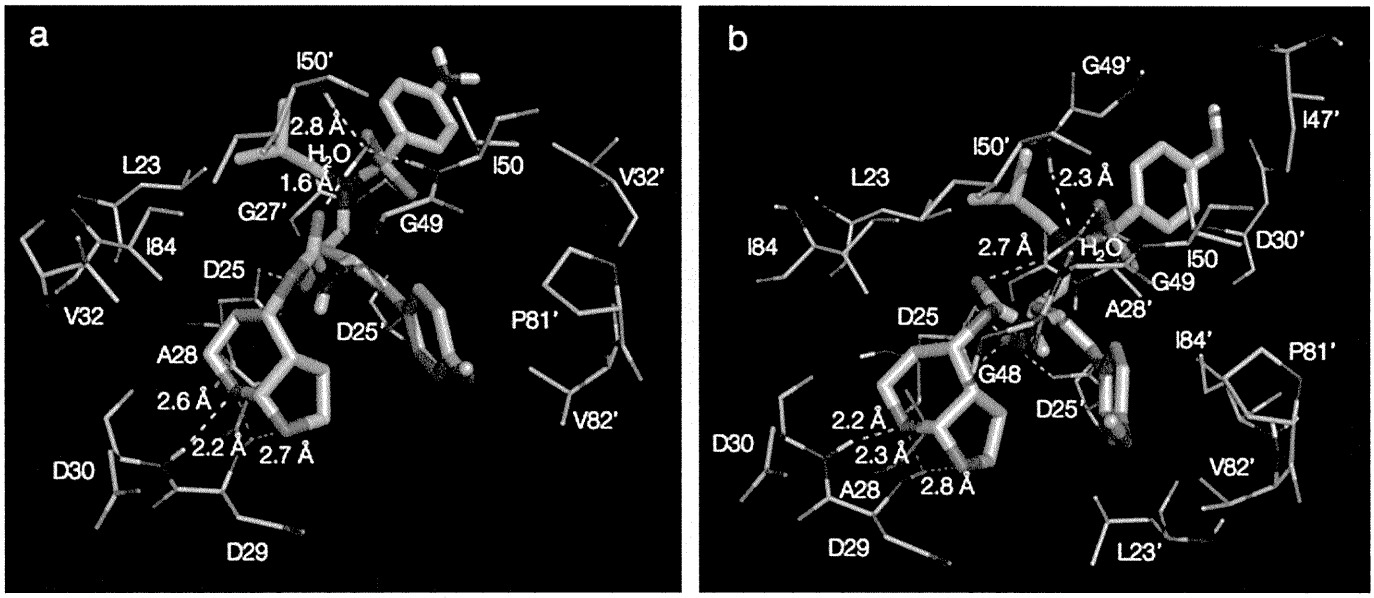

FIG. 7. Structural analysis of GRL-1388 and -1398 modeled into the active-site cavity of wild-type HIV-1 protease. GRL-1388 (a) and GRL-1398 (b) are shown as stick models (white color). Protease residues involved in either hydrogen bonding or hydrophobic interactions are highlighted in green. The distances for selected hydrogen bonds are shown. The novel Tp-THF functional group in both the compounds shows strong hydrogen bonding interactions with the backbone of residues Asp29 and Asp30.

tion was seen in two sets of selection experiments (Fig. 4 and 5; see Fig. S1 and S2 in the supplemental material), whereas A28S did not appear throughout the selection experiments with GRL-1388 or DRV. Although A28S substitution has been seen in HIV-1 selected with TMC-126 (36), GRL-98065 (1), and brecanavir (GW640385) (35), all of which contain the *bis*-THF moiety, the appearance of A28S has not been reported in the case of HIV-1 exposed to DRV *in vitro* (17) or *in vivo* (6, 24). Considering that both TMC-126 and GRL-1398 contain a methoxybenzene moiety but both DRV and GRL-1388 contain an aminobenzene moiety in the P2′ site, the presence of the methoxybenzene might be associated with the development of A28 substitution (Fig. 7b).

Amino acid substitutions in HIV-1 stoichiometrically and randomly occur, and the resulting amino acid substitutions in *in vitro* selection can vary from one experiment to another (34, 36). Thus, the results of a single selection experiment have to be confirmed with repeated selection experiments. In the present study, the selection experiment using HIV-1_{NL4-3} as a starting HIV-1 strain was conducted twice, and different profiles of amino acid substitutions were observed: the A28S substitution developed in the experiment II with GRL-1398, while it did not in the experiment I of the same compound (Fig. 4). Another selection experiment with GRL-1398 was planned; however, the selection experiment is, in general, labor-intensive and time-consuming. In fact, the selection experiment in the present study illustrated in Fig. 4 took more than 50 weeks each time. We thus performed the third selection experiment with a mixture of 10 $_{CL}$HIV-1_{MDR} variants as a starting virus population, expecting that highly GRL-1398-resistant HIV-1 variants would develop much sooner than when a single HIV-1 strain was used as a starting virus

TABLE 6. Interactions between wild type HIV-1 protease and GRL-1388 or -1398[a]

Compound	Amino acid residues and a bridging water involved in H bonding (no. of H bonds)	Total no. of H bonds	Amino acid residues involved in hydrophobic interactions (no. of hydrophobic interactions)	Total no. of hydrophobic interactions
DRV	D25 (1), G27 (1), D29 (2), D30 (1), D29′ (1), D30′ (1), water (2)	9	L23 (1), G27 (1), A28 (2), V32 (2), P81 (5), V82 (1), I84 (4), L23′ (1), D29′ (1), G49′ (3), G50′ (3), V82′ (1), I84′ (1)	26
GRL-1388	D25 (2), D29 (2), D30 (1), water (2)	7	L23 (1), A28 (4), D29 (1), V32 (2), G49 (5), I50 (1), I84 (2), G27′ (1), A28′ (6), V32′ (1), I50′ (1), P81′ (4), V82′ (2)	31
GRL-1398	D25 (2), D29 (2), D30 (1), D25′ (2), water (2)	8	L23 (1), D25 (1), A28 (1), D29 (2), D30 (3), G48 (1), G49 (3), I84 (2), L23′ (1), D25′ (1), G27′ (2), A28′ (3), D30′ (1), I47′ (1), G49′ (1), P81′ (4), V82′ (4), I84′ (2)	34

[a] The hydrogen bonding, as well as the hydrophobic interaction profiles of GRL-1388 and -1398 formed within the hydrophobic cavity of wild type HIV-1 protease, are shown along with those of DRV. The protease amino acid residues are listed, along with the numbers (in parentheses) of corresponding interactions. Note that GRL-1398 has relatively more hydrophobic interactions than GRL-1388, which should be one explanation for the greater potency of GRL-1398 against HIV-1. The two identical subunits that HIV-1 protease consists of were distinguished from each other by the use of a prime sign (′) at the upper right of each amino acid number.

population since multiple $_{CL}$HIV-1_{MDR} variants would undergo homologous recombination and also acquire amino acid substations *de novo* under the pressure of GRL-1398, resulting in quicker development of GRL-1398 resistance. In fact, using a mixture of eight multi-PI resistant clinical isolates, we successfully selected a highly DRV-resistant HIV-1 variant by 51 passages (68 weeks), although our group (17) and other groups (5) had failed to select such a variant using a single strain as a starting virus population. Indeed, in the third selection experiment, HIV-1 variants that replicated in the presence of 5 μM GRL-1388, DRV, and GRL-1398 appeared in 17, 21, and 29 weeks of selection periods, respectively.

One can assume that the amino acid positions, where secondary and further mutations occur, are affected under the influence of primary mutations. In the selection assay starting with 10 $_{CL}$HIV-1_{MDR} isolates, certain HIV-1 isolates most likely had already possessed various sets of amino acid substitutions in protease, some of which might have readily given replication advantages to the resulting GRL-1388- and DRV-resistant variants but not to GRL-1398-resistant variant. This should explain why the emergence of GRL-1398 resistance-associated mutations was delayed compared to the viruses selected with GRL-1388 or DRV. Moreover, homologous recombination among these 10 $_{CL}$HIV-1_{MDR} isolates might have given certain advantages in the speed for gaining resistance.

HIV-$1_{GRL1398\text{-}1\mu M^{Exp.I}}$ was more susceptible to DRV and GRL-1388 than was HIV-$1_{GRL1398\text{-}1\mu M^{Exp.II}}$ (Table 5). This susceptibility difference should stem from the difference in the amino acid substitutions obtained differently by the two variant populations. Both populations contained L10F and M46I substitutions; however, the former additionally had four amino acid substitutions and the latter had two substitutions. Both populations had compromised replication fitness compared to wild-type $HIV_{NL4\text{-}3}$, whereas both of them had a similarly significant advantages in replication in the presence of GRL-1398 (Fig. 6), proving that each set of amino acid substitutions conferred on the population significant levels of resistance to GRL-1398.

Modeling studies of GRL-1388 and -1398 docked against wild-type HIV-1 protease showed that the overall binding conformation of both compounds is similar (albeit not identical) to that of DRV. GRL-1398 shows more hydrogen bonds and hydrophobic interactions compared to GRL-1388. Structural analysis of GRL-1398 suggested that the potential extra hydrogen bonds with amide nitrogen atoms of Asp29′ and Asp30′ residues of the protease backbone could contribute to its greater potency. Based on this analysis, we postulate that these two hydrogen bonds with the backbone should be tolerant against mutations in the side chains from a wide spectrum of multidrug-resistant HIV-1 variants that we examined in comparison to either GRL-1388 or DRV. Due to the strong hydrogen bonds formed by GRL-1398 with the protease backbone, the overall binding profile of this compound is different from that of GRL-1388. This unique binding conformation of GRL-1398 is explained by the difference in the profiles of both GRL-1388 and -1398 with respect to their hydrophobic interactions in the protease active site.

ACKNOWLEDGMENTS

We thank Matthew L. Danish for helpful discussion and carefully reading the manuscript.

This study was supported in part by the Intramural Research Program of Center for Cancer Research, National Cancer Institute, National Institutes of Health (D.D. and H.M.); a grant from the National Institutes of Health (GM53386 to A.K.G.); a Grant-in-Aid for Scientific Research (Priority Areas to H.M.) from the Ministry of Education, Culture, Sports, Science, and Technology (Monbu-Kagakusho) of Japan (H.M.); and a Grant for Promotion of AIDS Research from the Ministry of Health, Labor, and Welfare (Kosei-Rodosho) of Japan (H.M.). This study utilized the computational resources of the Biowulf cluster at the National Institutes of Health.

REFERENCES

1. **Amano, M., et al.** 2007. A novel *bis*-tetrahydrofuranylurethane-containing nonpeptidic protease inhibitor (PI), GRL-98065, is potent against multiple-PI-resistant human immunodeficiency virus in vitro. Antimicrob. Agents Chemother. **51:**2143–2155.
2. **Bastiaens, P. I., and T. M. Jovin.** 1996. Microspectroscopic imaging tracks the intracellular processing of a signal transduction protein: fluorescent-labeled protein kinase C beta I. Proc. Natl. Acad. Sci. U. S. A. **93:**8407–8412.
3. **Bastiaens, P. I., I. V. Majoul, P. J. Verveer, H. D. Soling, and T. M. Jovin.** 1996. Imaging the intracellular trafficking and state of the AB5 quaternary structure of cholera toxin. EMBO J. **15:**4246–4253.
4. **Collaborative Computational Project, Number 4.** 1994. The CCP4 suite: programs for protein crystallography. Acta Crystallogr. **D50:**760–763.
5. **De Meyer, S., et al.** 2005. TMC114, a novel human immunodeficiency virus type 1 protease inhibitor active against protease inhibitor-resistant viruses, including a broad range of clinical isolates. Antimicrob. Agents Chemother. **49:**2314–2321.
6. **De Meyer, S., et al.** 2008. Resistance profile of darunavir: combined 24-week results from the POWER trials. AIDS Res. Hum. Retrovir. **24:**379–388.
7. **Fang, G., B. Weiser, A. Visosky, T. Moran, and H. Burger.** 1999. PCR-mediated recombination: a general method applied to construct chimeric infectious molecular clones of plasma-derived HIV-1 RNA. Nat. Med. **5:**239–242.
8. **Friesner, R. A., et al.** 2004. Glide: a new approach for rapid, accurate docking and scoring. 1. Method and assessment of docking accuracy. J. Med. Chem. **47:**1739–1749.
9. **Friesner, R. A., et al.** 2006. Extra precision glide: docking and scoring incorporating a model of hydrophobic enclosure for protein-ligand complexes. J. Med. Chem. **49:**6177–6196.
10. **Gatanaga, H., et al.** 2002. Amino acid substitutions in Gag protein at non-cleavage sites are indispensable for the development of a high multitude of HIV-1 resistance against protease inhibitors. J. Biol. Chem. **277:**5952–5961.
11. **Ghosh, A. K., et al.** 2008. Design and synthesis of stereochemically defined novel spirocyclic P2-ligands for HIV-1 protease inhibitors. Org. Lett. **10:** 5135–5138.
12. **Ghosh, A. K., et al.** 2008. Flexible cyclic ethers/polyethers as novel P2-ligands for HIV-1 protease inhibitors: design, synthesis, biological evaluation, and protein-ligand X-ray studies. J. Med. Chem. **51:**6021–6033.
13. **Ghosh, A. K., et al.** 2010. Synthesis and biological evaluation of novel allophenylnorstatine-based HIV-1 protease inhibitors incorporating high-affinity P2-ligands. Bioorg. Med. Chem. Lett. **20:**1241–1246.
14. **Ghosh, A. K., et al.** 2008. Potent HIV-1 protease inhibitors incorporating meso-bicyclic urethanes as P2-ligands: structure-based design, synthesis, biological evaluation and protein-ligand X-ray studies. Org. Biomol. Chem. **6:**3703–3713.
15. **Ghosh, A. K., et al.** 1998. Potent HIV protease inhibitors incorporating high-affinity P2-ligands and (*R*)-(hydroxyethylamino)sulfonamide isostere. Bioorg. Med. Chem. Lett. **8:**687–690.
16. **Ghosh, A. K., S. Leshchenko, and M. Noetzel.** 2004. Stereoselective photochemical 1,3-dioxolane addition to 5-alkoxymethyl-2(5*H*)-furanone: synthesis of *bis*-tetrahydrofuranyl ligand for HIV protease inhibitor UIC-94017 (TMC-114). J. Org. Chem. **69:**7822–7829.
17. **Koh, Y., et al.** 2010. In vitro selection of highly darunavir-resistant and replication-competent HIV-1 variants by using a mixture of clinical HIV-1 isolates resistant to multiple conventional protease inhibitors. J. Virol. **84:** 11961–11969.
18. **Koh, Y., et al.** 2007. Potent inhibition of HIV-1 replication by novel non-peptidyl small molecule inhibitors of protease dimerization. J. Biol. Chem. **282:**28709–28720.
19. **Koh, Y., et al.** 2003. Novel *bis*-tetrahydrofuranylurethane-containing nonpeptidic protease inhibitor (PI) UIC-94017 (TMC114) with potent activity against multi-PI-resistant human immunodeficiency virus in vitro. Antimicrob. Agents Chemother. **47:**3123–3129.
20. **Lohse, N., et al.** 2007. Survival of persons with or without HIV infection in Denmark, 1995–2005. Ann. Intern. Med. **146:**87–95.
21. **Madruga, J. V., et al.** 2007. Efficacy and safety of darunavir-ritonavir com-

pared with that of lopinavir-ritonavir at 48 weeks in treatment-experienced, HIV-infected patients in TITAN: a randomised controlled phase III trial. Lancet **370:**49–58.
22. **Maeda, K., et al.** 2001. Novel low-molecular-weight spirodiketopiperazine derivatives potently inhibit R5 HIV-1 infection through their antagonistic effects on CCR5. J. Biol. Chem. **276:**35194–35200.
23. **Miller, J. F., et al.** 2006. Ultra-potent P1 modified arylsulfonamide HIV protease inhibitors: the discovery of GW0385. Bioorg. Med. Chem. Lett. **16:**1788–1794.
24. **Mitsuya, Y., T. F. Liu, S. Y. Rhee, W. J. Fessel, and R. W. Shafer.** 2007. Prevalence of darunavir resistance-associated mutations: patterns of occurrence and association with past treatment. J. Infect. Dis. **196:**1177–1179.
25. **Ortiz, R., et al.** 2008. Efficacy and safety of once-daily darunavir/ritonavir versus lopinavir/ritonavir in treatment-naive HIV-1-infected patients at week 48. AIDS **22:**1389–1397.
26. Reference deleted.
27. **Sekar, R. B., and A. Periasamy.** 2003. Fluorescence resonance energy transfer (FRET) microscopy imaging of live cell protein localizations. J. Cell Biol. **160:**629–633.
28. **Shirasaka, T., et al.** 1995. Emergence of human immunodeficiency virus type 1 variants with resistance to multiple dideoxynucleosides in patients receiving therapy with dideoxynucleosides. Proc. Natl. Acad. Sci. U. S. A. **92:**2398–2402.
29. **Szczesna-Skorupa, E., B. Mallah, and B. Kemper.** 2003. Fluorescence resonance energy transfer analysis of cytochromes P450 2C2 and 2E1 molecular interactions in living cells. J. Biol. Chem. **278:**31269–31276.
30. **Tamiya, S., S. Mardy, M. F. Kavlick, K. Yoshimura, and H. Mistuya.** 2004. Amino acid insertions near Gag cleavage sites restore the otherwise compromised replication of human immunodeficiency virus type 1 variants resistant to protease inhibitors. J. Virol. **78:**12030–12040.
31. **Tie, Y., et al.** 2004. High resolution crystal structures of HIV-1 protease with a potent non-peptide inhibitor (UIC-94017) active against multidrug-resistant clinical strains. J. Mol. Biol. **338:**341–352.
32. **Tojo, Y., et al.** 2010. Novel protease inhibitors (PIs) containing macrocyclic components and 3(*R*),3a(*S*),6a(*R*)-*bis*-tetrahydrofuranylurethane that are potent against multi-PI-resistant HIV-1 variants in vitro. Antimicrob. Agents Chemother. **54:**3460–3470.
33. **Walensky, R. P., et al.** 2006. The survival benefits of AIDS treatment in the United States. J. Infect. Dis. **194:**11–19.
34. **Watkins, T., W. Resch, D. Irlbeck, and R. Swanstrom.** 2003. Selection of high-level resistance to human immunodeficiency virus type 1 protease inhibitors. Antimicrob. Agents Chemother. **47:**759–769.
35. **Yates, P. J., et al.** 2006. In vitro development of resistance to human immunodeficiency virus protease inhibitor GW640385. Antimicrob. Agents Chemother. **50:**1092–1095.
36. **Yoshimura, K., et al.** 2002. A potent human immunodeficiency virus type 1 protease inhibitor, UIC-94003 (TMC-126), and selection of a novel (A28S) mutation in the protease active site. J. Virol. **76:**1349–1358.
37. **Yoshimura, K., et al.** 1999. JE-2147: a dipeptide protease inhibitor (PI) that potently inhibits multi-PI-resistant HIV-1. Proc. Natl. Acad. Sci. U. S. A. **96:**8675–8680.

622 J. Med. Chem. 2011, 54, 622–634
DOI: 10.1021/jm1012787

Journal of
Medicinal
Chemistry
Article

Design and Synthesis of Potent HIV-1 Protease Inhibitors Incorporating Hexahydrofuropyranol-Derived High Affinity P_2 Ligands: Structure−Activity Studies and Biological Evaluation

Arun K. Ghosh,*[,†,‡] Bruno D. Chapsal,[†] Abigail Baldridge,[†] Melinda P. Steffey,[†] D. Eric Walters,[§] Yasuhiro Koh,[∥,⊥] Masayuki Amano,[∥,⊥] and Hiroaki Mitsuya[∥,⊥,#]

[†]*Department of Chemistry, and* [‡]*Department of Medicinal Chemistry, Purdue University, West Lafayette, Indiana 47907, United States,* [§]*Department of Biochemistry and Molecular Biology, Rosalind Franklin University of Medicine and Science, North Chicago, Illinois 60064, United States,* [∥]*Department of Hematology, and* [⊥]*Department of Infectious Diseases, Kumamoto University School of Medicine, Kumamoto 860-8556, Japan, and* [#]*Experimental Retrovirology Section, HIV and AIDS Malignancy Branch, National Cancer Institute, Bethesda, Maryland 20892, United States*

Received October 4, 2010

The design, synthesis, and evaluation of a new series of hexahydrofuropyranol-derived HIV-1 protease inhibitors are described. We have designed a stereochemically defined hexahydrofuropyranol-derived urethane as the P2-ligand. The current ligand is designed based upon the X-ray structure of **1a**-bound HIV-1 protease. The synthesis of (3a*S*,4*S*,7a*R*)-hexahydro-2*H*-furo[2,3-*b*]pyran-4-ol, (−)-**7**, was carried out in optically active form. Incorporation of this ligand provided inhibitor **35a**, which has shown excellent enzyme inhibitory activity and antiviral potency. Our structure−activity studies have indicated that the stereochemistry and the position of oxygens in the ligand are important to the observed potency of the inhibitor. Inhibitor **35a** has maintained excellent potency against multidrug-resistant HIV-1 variants. An active site model of **35a** was created based upon the X-ray structure of **1b**-bound HIV-1 protease. The model offers molecular insights regarding ligand-binding site interactions of the hexahydrofuropyranol-derived novel P2-ligand.

Introduction

HIV-1 protease inhibitors are critical components of highly active antiretroviral therapy (HAART[a]).[1−3] The HAART treatment regimens significantly reduced HIV/AIDS-related mortality.[4,5] However, the rapid emergence of drug-resistant HIV-1 strains and the appearance of cross-resistance are severely limiting long-term treatment options.[6−8] An estimated 10−25% of newly infected patients harbor at least one viral strain that is resistant to current medications.[9−11] In addition, PI regimens suffer from a number of other drawbacks including high pill burden, treatment cost, poor ADMET properties, debilitating side effects, and toxicity issues.[12] Therefore, the development of novel PIs with broad-spectrum activity against multidrug-resistant HIV-1 variants remains a major therapeutic objective.[13]

In our continuing interest to develop novel protease inhibitors (PI) with broad-spectrum activity against multidrug-resistant HIV-1 variants, we have reported a series of PIs including PIs **1a**, **1b**, **2**, and **3**.[14−16] These inhibitors exhibited excellent antiviral activity against multidrug-resistant HIV-1 variants. Darunavir (TMC-114, Figure 1) has been recently approved by the FDA.[17,18] It has displayed a high genetic barrier to resistance and retained high potency against multidrug resistant HIV-1 strains. It has been demonstrated that resistance to **1a** is significantly delayed compared to other approved PIs.[19−21]

Our structure-based design of **1a** and other PIs is inspired by the premise that an inhibitor engaged in multiple interactions, especially hydrogen bonding with the HIV protease backbone atoms, should retain these affinities with mutant strains.[22] As the enzyme backbone conformation is only minimally distorted when mutations occur, backbone atoms−PI interactions are likely maintained, therefore sustaining the inhibitor affinity and potency. Inhibitor **1a**'s superb resistance profile likely originates from the extensive interactions the inhibitor makes within the HIV-1 protease's binding site and particularly with the backbone atoms of the enzyme.[22−24] Extensive studies of **1a**-bound HIV-1 protease crystal structures have consistently revealed tight hydrogen bonding between the inhibitor and the protease backbone.[23−25] The stereochemically defined bis-tetrahydrofuran (bis-THF) P_2 ligand in **1a** forms a strong hydrogen bonding network between its two cyclic ether oxygens and the backbone amide NH bonds of the protease residues, Asp29 and Asp30.[22] These observations likely provide explanations for **1a**'s outstanding antiviral activity. Not surprisingly, several other protease inhibitors featuring the bis-THF as the P_2 ligand have exhibited equally impressive antiviral activities and resistance profiles.[22,26]

The bis-THF ligand represents an intriguing pharmacophoric scaffold for the development of PIs to combat drug resistance. To further optimize the bis-THF structural template, we have now investigated ligands that could enhance the backbone-binding as well as improve hydrophobic interactions with the protease active site. The X-ray structure of **1a**-bound HIV-1 protease has shown a distance of about 3.0−3.2 Å

*To whom correspondence should be addressed. Phone: (765)-494-5323. Fax: (765)-496-1612. E-mail: akghosh@purdue.edu.

[a]Abbreviations: bis-THF, bis-tetrahydrofuran; Cp-THF, cyclopentanyltetrahydrofuran; Tp-THF, tetrahydropyranyltetrahydrofuran; PI, protease inhibitor; HAART, highly active antiretroviral therapy; APV, amprenavir; DRV, darunavir; SQV, saquinavir; IDV, indinavir; LPV, lopinavir; RTV, ritonavir; ATV, atazanavir.

 Published on Web 12/31/2010

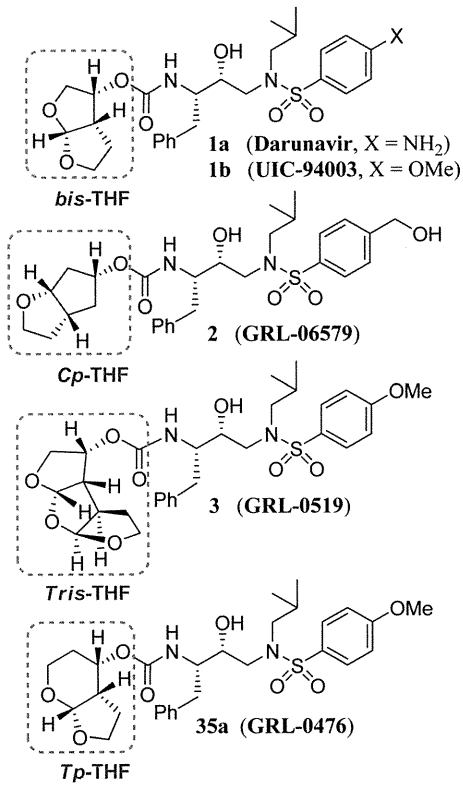

Figure 1. Structures of inhibitors **1**–**3** and **35a**.

between the bis-THF cyclic oxygens and the Asp30 NH amide bond, while a shorter 2.9 Å distance was observed with the Asp29 NH bond.[23,25] In order to maximize and promote closer hydrogen bonding with the Asp30 backbone NH bond, we thought a larger ring on the P_2 ligand should increase the dihedral angle of the bicyclic acetal, bring the oxygen closer, give more flexibility to the structure, and offer a more optimal alignment of the cyclic oxygen with the Asp30 NH bond. Such factors could realistically promote tighter hydrogen bonding with the Asp30 backbone NH bond. Besides, this extra methylene group in the "inner" ring would also provide more favorable van der Waals interactions within the hydrophobic pocket created by Ile47, Val32, Ile84, Leu76, and Ile50′ residues in the protease S_2 subsite. In addition, a larger ring could potentially lead to better flexibility and adaptability to protease mutations. Herein, we report the design, synthesis, and biological evaluation of a series of highly potent PIs that combined a (*R*)-hydroxyethylsulfonamide isostere with the furopyranol ligand (−)-**7**. Among all inhibitors of the series, **35a** showed the most impressive inhibitory and antiviral activity (K_i = 2.7 pM, IC_{50} = 0.5 nM). Moreover, inhibitor **35a** was evaluated against a panel of multidrug-resistant HIV-1 viruses. It retained potent activity against a variety of multidrug-resistant clinical HIV-1 strains with EC_{50} values in low nanomolar range, which is superior to other PIs and comparable to **1a**. Modeling of **35a** based upon the X-ray structure of **1b**-bound HIV-1 protease active site has provided critical molecular insight into the ligand-binding site interactions.

Chemistry

The synthesis of enantiomerically pure (3a*S*,4*S*,7a*R*)-hexahydro-2*H*-furo[2,3-*b*]pyran-4-ol is shown in Scheme 1. It was achieved starting from known enantiomerically pure lactone **4**.[27] Lactone **4** was reduced into the corresponding

Scheme 1. Synthesis of Ligand (−)-**7** and Its Respective Enantiomer (+)-**7**

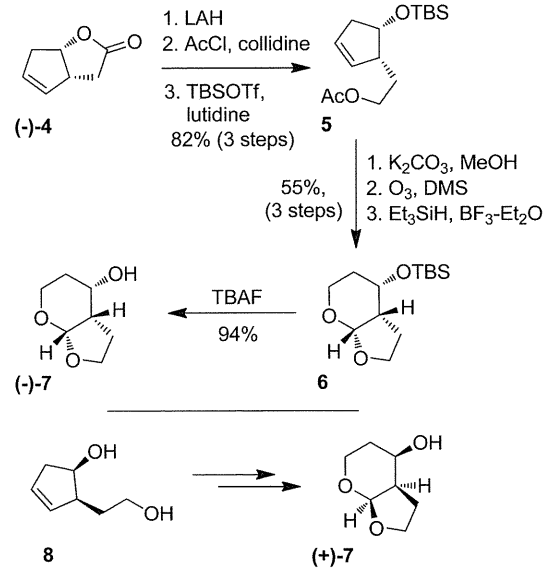

diol using lithium aluminum hydride in 95% yield. Selective monoacetylation at the primary alcohol using AcCl and 2,4,6-collidine at −78 °C[28] and subsequent silylation of the remaining free hydroxyl furnished intermediate **5** in 86% yield (two steps). Removal of the acetate group, followed by ozonolysis of the olefin, furnished a bicyclic bis-acetal intermediate. Reduction of the hemiacetal moiety using Et_3SiH and BF_3–Et_2O afforded bicyclic intermediate **6** in 55% yield in three steps. Removal of the silyl group with TBAF in THF furnished the desired hexahydrofuropyran-4-ol ligand (−)-**7**.

To demonstrate the importance of the absolute stereochemistry of the bicyclic structure of ligand (−)-**7**, its corresponding enantiomer (+)-**7** was synthesized starting from intermediate **8** (Scheme 1). Intermediate **8** was synthesized by an enzyme-catalyzed desymmetrization of cyclopentene *meso*-diacetate followed by a Claisen rearrangement step.[27b,29] The resulting diester was reduced by LAH to provide **8**. It was used for the synthesis of (+)-**7** and subjected to the same synthetic sequence applied from lactone (−)-**4** in the synthesis of (−)-**7** (Scheme 1). To examine the importance of each of the two cyclic ether oxygens in the furopyranol ligand (−)-**7**, we prepared the corresponding cyclohexane and cyclopentane derivatives (Schemes 2 and 3).

The synthesis of 4-hydroxyoctahydrobenzofuran ligand (−)-**12** is shown in Scheme 2. Reaction of diazocyclohexanedione **9**[30] with ethyl vinyl ether in presence of a catalytic amount of $Rh_2(OAc)_4$ at 23 °C gave derivative **10**.[31] Hydrogenation of the ketofuran in the presence of Pd/C under H_2 (1 atm) furnished the corresponding crude ketone **11** as a 9:1 mixture of diastereoisomers. A one-pot procedure involving L-selectride reduction of the ketone followed by Et_3SiH/TMSOTf-promoted reduction of the acetal furnished the racemic alcohol (±)-**12** (71% from **10**). Enzymatic resolution of (±)-**12** using lipase Amano PS-30 provided the desired enantiopure alcohol (−)-**12** (98.8% ee by chiral HPLC analysis of the 2,4-dinitrobenzoate derivative), after ~55% conversion to the acetate.

The synthesis of cyclopentapyranol ligand (−)-**18** is shown in Scheme 3. Pentanone **14** was treated with LDA and then reacted with *tert*-butyldimethylsilyloxypropionaldehyde[32]

Scheme 2. Synthesis of Furocyclohexanol P_2 Ligand (−)-**12**

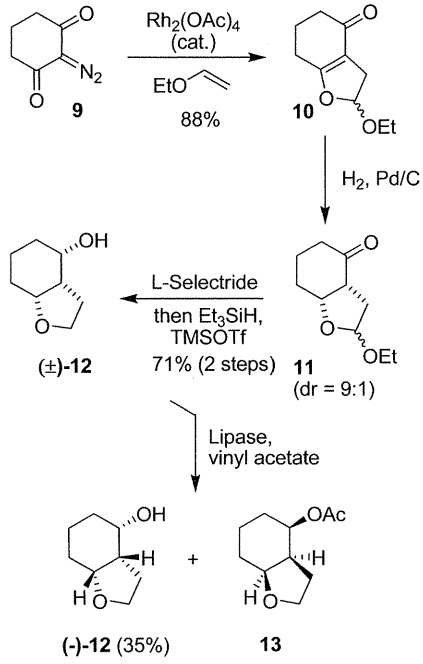

Scheme 3. Syntheses of Ligands (−)-**18** and (−)-**19**

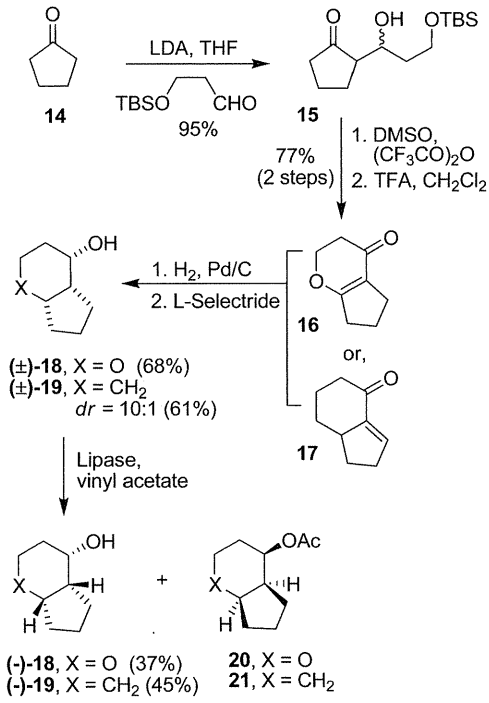

to furnish intermediate **15** (dr 3:1) in 95% yield. A DMSO-TFAA promoted oxidation of the free hydroxy group followed by TFA-promoted cyclocondensation furnished the bicyclic α,β-unsaturated ketone **16**. Hydrogenation in presence of 10% Pd/C followed by L-selectride reduction of the ketone gave racemic alcohol (±)-**18** as a single diastereomer in 68% yield over two steps. Lipase-catalyzed resolution of the alcohol provided enantiomerically pure alcohol (−)-**18**. For the synthesis of a P2 ligand devoid of any cyclic oxygen, known tetrahydroindanone **17**[33] was similarly hydrogenated in presence of 10% Pd/C to give the corresponding bicyclic ketone. Accordingly, L-selectride-promoted reduction of the

Scheme 4. Synthesis of Hexahydrofuro[3,4-*b*]pyran-4-ol Ligand **25**

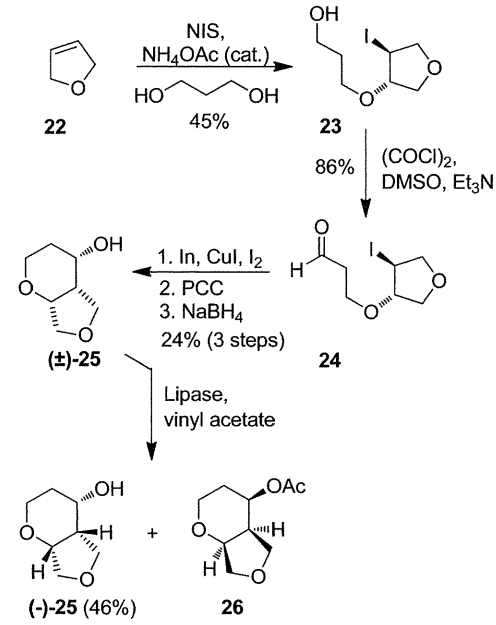

ketone provided the corresponding alcohol (dr = 10:1, as observed by ^1H and ^{13}C NMR). Lipase-mediated resolution of the major *cis*-alcohol gave the respective chiral ligand (−)-**19** (90% ee determined by chiral HPLC).

Since the introduction of a six-membered ring in the P_2 ligand structure may introduce more structural flexibility, we set out to explore ligands in which the cyclic oxygens were moved to adjacent positions. Such ligands would also demonstrate the importance of the oxygen positions in the bicyclic structure of ligand (−)-**7**. Thus, isomeric ligand **25** was synthesized with the furan oxygen moved to its vicinal position. The synthesis of 4-hydroxyhexahydro-2*H*-furo[3,4-*b*]pyran **25** is shown in Scheme 4. Iodoalkoxylation of the 2,5-dihydrofuran **22** using propanediol in the presence of *N*-iodosuccinimide and catalytic NH_4OAc provided iodo alcohol **23**. Swern oxidation gave aldehyde **24** in 86% yield. An intramolecular Barbier-type reaction was then conducted using indium in the presence of copper(I) iodide and iodine to furnish a mixture of diastereoisomeric alcohols.[34] Oxidation followed by stereoselective reduction using $NaBH_4$ furnished the racemic *cis,cis*-bicyclic alcohol (±)-**25** as the sole product. Lipase-mediated resolution finally gave the enantiomerically pure alcohol **25**.

To ascertain the importance of the position of the urethane in (−)-**7**, we have synthesized hexahydrofuropyran-5-ol ligand **30** shown in Scheme 5. The free hydroxyl on the pyran ring was moved to the C3 position. The synthesis was accomplished starting from enantiomerically pure bis-THF ligand **27** synthesized by us previously.[35] Dess−Martin oxidation of **27** provided the corresponding ketone. Homologation of the resulting ketone using trimethylsilyldiazomethane in the presence of $AlMe_3$ followed by treatment of the crude mixture with TBAF and acetic acid provided furanopyranone **29**. Stereoselective reduction of ketone **29** using L-selectride furnished alcohol **30** as a mixture of inseparable diastereoisomers (dr = 5:1). Both isomers were separated after formation of the corresponding activated mixed carbonate **31g**.

The synthesis of the protease inhibitors was accomplished in a two-step sequence shown in Schemes 6 and 7. Each ligand alcohol synthesized above was reacted with 4-nitrophenyl

Scheme 5. Synthesis of Hexahydrofuro[2,3-*b*]pyran-5-ol Ligand **30**

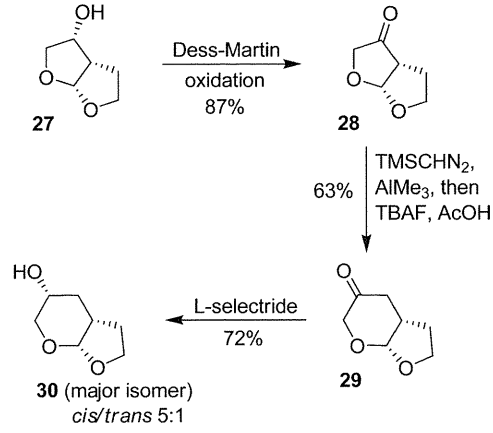

Scheme 6. Synthesis of Activated Mixed Carbonates **31a–g**

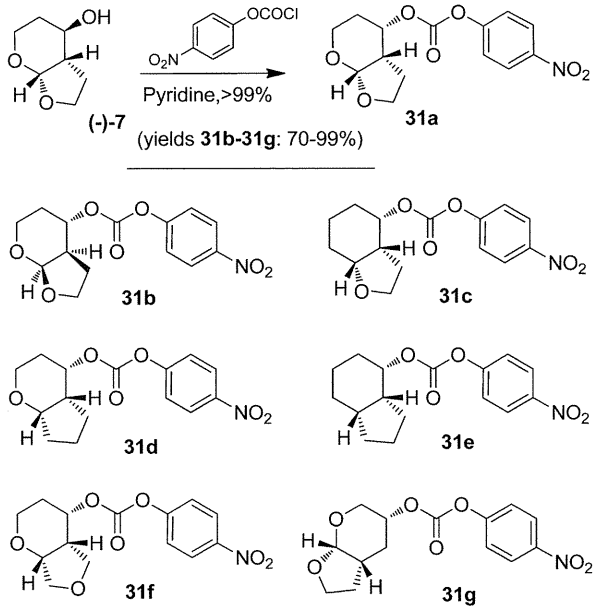

chloroformate in the presence of pyridine to form mixed activated carbonates **31a–g** in 70–99% yield. The syntheses of the corresponding protease inhibitors were achieved by coupling the mixed activated carbonates with previously reported hydroxyethylsulfonamide isosteres **32–34** (Scheme 7).[15,35] The syntheses of various HIV-PIs containing the Tp-THF (−)-**7** were achieved by respectively treating the Boc-protected isosteres **32–34** with TFA in CH_2Cl_2 and subsequently by coupling the resulting free amine isosteres with activated mixed carbonate **31a** in THF/CH_3CN in the presence of Et_3N. The corresponding inhibitors **35a**, **36**, and **37** were obtained in good yields (Scheme 7). Inhibitors **35b–g** were made in a similar manner.

Results and Discussion

As mentioned above, our preliminary modeling suggested that a hexahydrofuropyranol (−)-**7** ligand may interact with backbone atoms and residues in the protease S2-site. All inhibitors in Table 1 were evaluated in enzyme inhibitory assays following a protocol described by Toth and Marshall.[36] Inhibitors that showed potent K_i values were further evaluated through in vitro antiviral assays. As can be seen, inhibitor **35a**,

Scheme 7. Syntheses of Inhibitors **35a–g**, **36**, and **37**

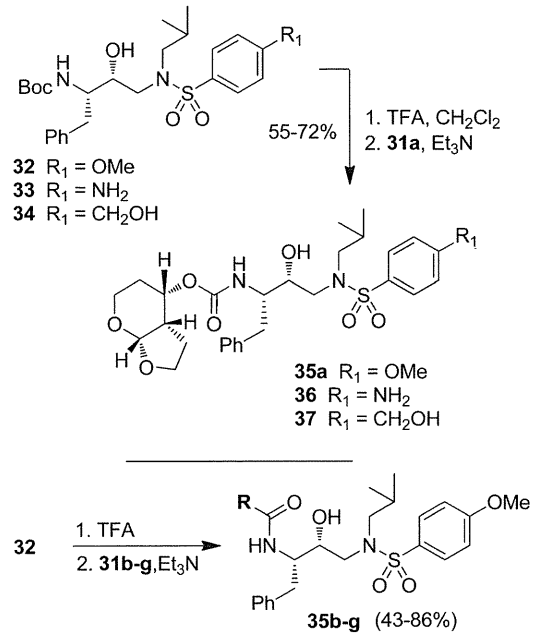

with Tp-THF (−)-**7**, exhibited an enzyme K_i value of 2.7 pM. Antiviral activity of **35a** and other inhibitors were determined in MT-2 human-T-lymphoid cells exposed to HIV-1_{LAI}.[19] As shown, **35a** has displayed remarkable antiviral potency (IC_{50} = 0.5 nM), comparable to those of PIs **1a** and **1b**. The bicyclic ring stereochemistry of the P_2 ligand proved to be important as inhibitor **35b**, with enantiomeric ligand (+)-**7**, displayed a significant reduction in enzyme inhibitory potency (>20-fold increase in K_i) as well as antiviral activity (IC_{50} = 19 nM).

To probe the importance of the cyclic ether oxygens in the bicyclic structure of (−)-**7**, inhibitors **35c–e** were synthesized and evaluated. As shown, inhibitor **35c**, with a cyclohexane ring in place of the tetrahydropyran ring, only displayed a 2-fold reduction in K_i values but a 16-fold decrease in antiviral activity compared to inhibitor **35a**. A more dramatic loss of enzymatic potency was observed with compound **35d** with a cyclopentane ring in place of a THF ring in the P2 ligand. The K_i value dropped to 1.43 nM. Inhibitor **35e**, which lacks both cyclic ether oxygens, displayed even lower K_i and no appreciable antiviral activity. Those results clearly demonstrated the critical role of both cyclic ether oxygens in ligand (−)-**7**. Furthermore, the difference of activity observed between **35a** and **35c** suggests that the O1 oxygen on the THF-ring of (−)-**7** exerts a stronger interaction with the enzyme compared to the pyran oxygen. Inhibitor **35f**, in which the THF-oxygen of the P_2 ligand is located at a vicinal position, also exhibited a substantial loss of potency (i.e., K_i = 5.3 nM) and no antiviral activity. These results corroborated our previous observations with the bis-THF ligand in PIs **1a** and **1b**. The THF-oxygen in (−)-**7** likely has a stronger hydrogen bonding interaction with the Asp29 backbone NH and may form a weak hydrogen bond with Asp30, in the S_2 subsite of the HIV protease. We have investigated the position of the urethane oxygen on the bicyclic ligand in inhibitor **35g**. This has resulted in a substantial loss of protease inhibitory activity. Furthermore, we have examined the potency enhancing effect of the Tp-THF ligand with various hydroxyethylsulfonamide isosteres to give inhibitors **36** and **37**. The 4-methoxysulfonamide derivative **35a** appears to be the most potent inhibitor in

Table 1. Enzymatic Inhibitory and Antiviral Activity of Compounds **35a–g**, **36**, and **37**[b]

Entry	Inhibitor	K_i (nM)	IC_{50} (μM)[a]
1	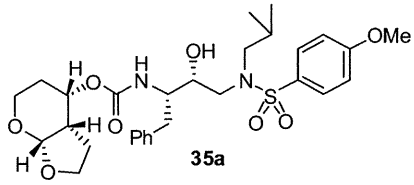 **35a**	0.0027	0.0005
2	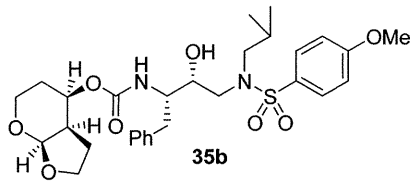 **35b**	0.068	0.019
3	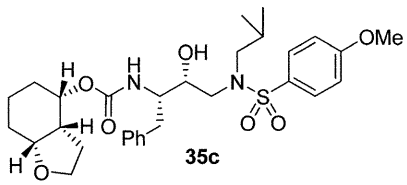 **35c**	0.005	0.008
4	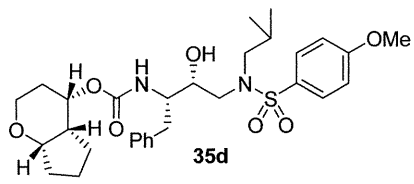 **35d**	1.43	--
5	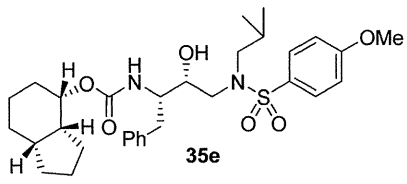 **35e**	9	>1 μM
6	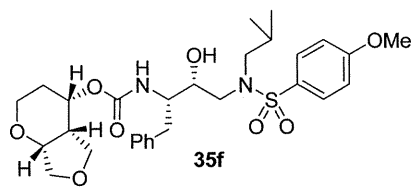 **35f**	5.3	>1 μM
7	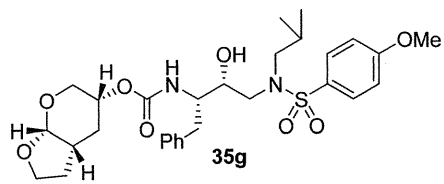 **35g**	0.11	--
8	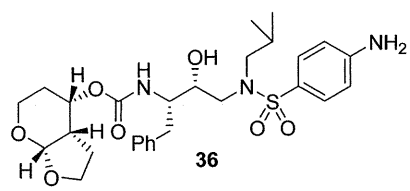 **36**	0.010	0.0065
9	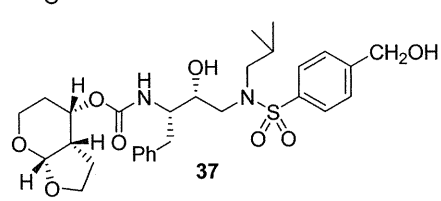 **37**	0.085	0.0045

[a] Values are the mean of at least two experiments. [b] Human T-lymphoid (MT-2) cells (2×10^3) were exposed to 100 $TCID_{50}$ of HIV-1_{LAI} and cultured in the presence of each PI, and IC_{50} values were determined using the MTT assay. The IC_{50} values of amprenavir (APV), saquinavir (SQV), and indinavir (IDV) were 0.03, 0.015, and 0.03 μM, respectively.